Journal of Computer-Aided Molecular Design, 10 (1996) 461–478
ESCOM



J-CAMD 355

# The agonistic binding site at the histamine $H_2$ receptor. I. Theoretical investigations of histamine binding to an oligopeptide mimicking a part of the fifth transmembrane α-helix

Paul H.J. Nederkoorn[a], Joop H. van Lenthe[b], Henk van der Goot[a], Gabriëlle M. Donné-Op den Kelder[a] and Henk Timmerman[a,*]

[a]*Department of Pharmacochemistry, Leiden/Amsterdam Center for Drug Research (LACDR), Vrije Universiteit, De Boelelaan 1083, 1081 HV Amsterdam, The Netherlands*
[b]*Theoretical Chemistry Group, Debije Institute, Utrecht University, Padualaan 14, 3584 CH Utrecht, The Netherlands*

Received 26 February 1996
Accepted 28 May 1996

*Keywords:* α-helical model system; Conformational analysis; Counterpoise method; Hartree–Fock calculations; Histamine $H_2$ receptor; Molecular mechanics

## Summary

Mutation studies on the histamine $H_2$ receptor were reported by Gantz et al. [J. Biol. Chem., 267 (1992) 20840], which indicate that both the mutation of the fifth transmembrane $Asp^{186}$ (to $Ala^{186}$) alone or in combination with $Thr^{190}$ (to $Ala^{190}$) maintained, albeit partially, the cAMP response to histamine. Recently, we have shown that histamine binds to the histamine $H_2$ receptor as a monocation in its proximal tautomeric form, and, moreover, we suggested that a proton is donated from the receptor towards the tele-position of the agonist, thereby triggering the biological effect [Nederkoorn et al., J. Mol. Graph., 12 (1994) 242; Eriks et al., Mol. Pharmacol., 44 (1993) 886]. These findings result in a close resemblance with the catalytic triad (consisting of Ser, His and Asp) found in serine proteases. $Thr^{190}$ resembles a triad's serine residue closely, and could also act as a proton donor. However, the mutation of $Thr^{190}$ to $Ala^{190}$ – the latter is unable to function as a proton donor – does not completely abolish the agonistic cAMP response. At the fifth transmembrane α-helix of the histamine $H_2$ receptor near the extracellular surface, another amino acid is present, i.e. $Tyr^{182}$, which could act as a proton donor. Furthermore, $Tyr^{182}$ lies within the proximity of $Asp^{186}$, so an alternative couple of amino acids, $Tyr^{182}$ and $Asp^{186}$, could constitute the histamine binding site at the fifth α-helix instead of the (mutated) couple $Asp^{186}$ and $Thr^{190}$. In the first part of our present study, this hypothesis is investigated with the aid of an oligopeptide with an α-helical backbone, which represents a part of the fifth transmembrane helix. Both molecular mechanics and ab initio data lead to the conclusion that the $Tyr^{182}/Asp^{186}$ couple is most likely to act as the binding site for the imidazole ring present in histamine.

## Introduction

*Proton transfers and mutation studies*

Several years ago, Weinstein et al. [1] derived a model for the activation of the histamine $H_2$ receptor. In this model, the heterocycle of an agonist binds via two H-bonds to the receptor, whereas the cationic side chain is assumed to interact with a negatively charged receptor site (Fig. 1A). Subsequently, a double proton transfer is thought to trigger the agonistic response. This activation process consists of a proton donation from the receptor towards the heterocycle present in agonists, followed by a proton donation from the agonist towards the receptor (Fig. 1B). Neutralization of the histamine side chain is assumed to induce the double proton transfer process. With this theory in mind, Gantz et al. [2] performed a series of mutation studies on the canine histamine $H_2$ receptor. The amino acids selected for the mutations were chosen on the basis of earlier mutation studies on the catecholamine $\beta_2$ receptor and the presumed structural

*To whom correspondence should be addressed.

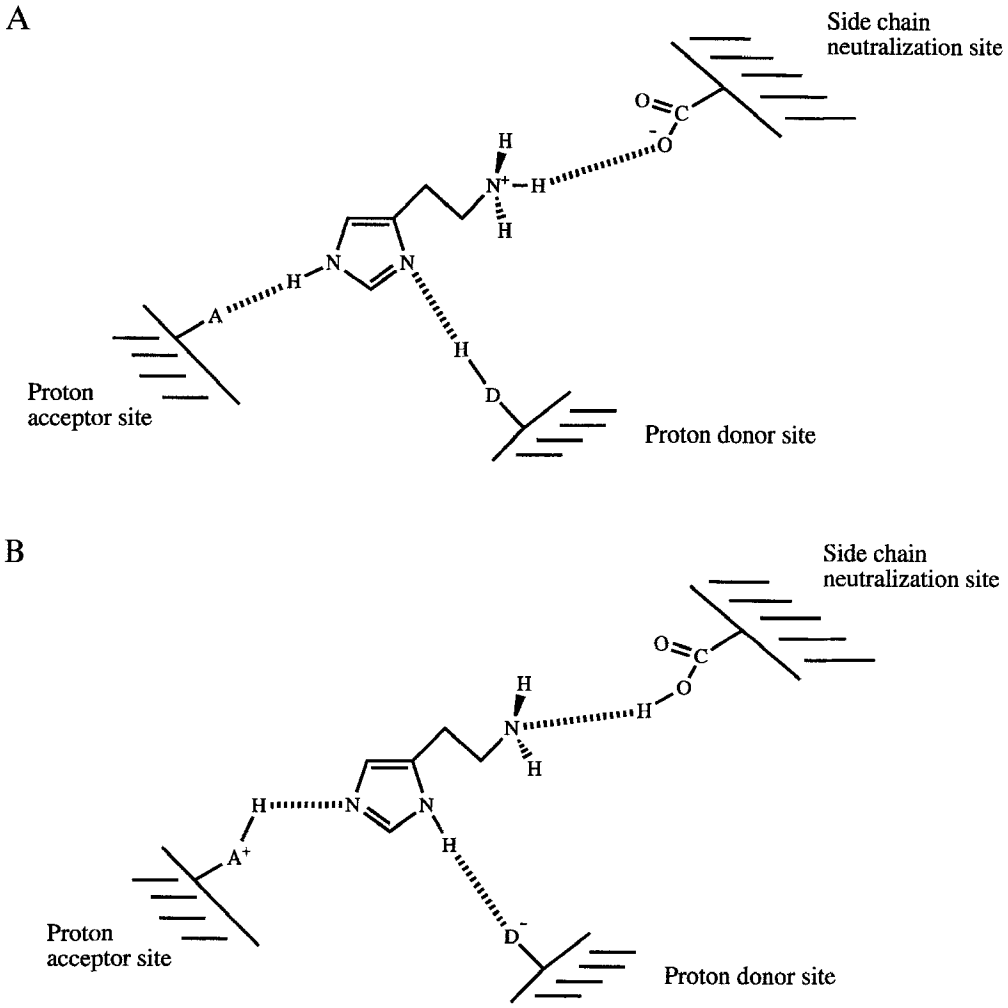


Fig. 1. Activation of the histamine $H_2$ receptor by a double proton transfer involving the heterocyclic ring of histamine according to Weinstein et al. [1]: initial (A) and final (B) situation. See text for further details.

homology between the histamine $H_2$ receptor and the $\beta_2$ adrenoceptor. $Asp^{98}$ from the third transmembrane α-helix was assumed to neutralize the side chain of the histamine, whereas $Asp^{186}$ and $Thr^{190}$ from the fifth transmembrane α-helix were considered as potential candidates for binding the imidazole ring and to play a crucial role in the activation process (Fig. 1). The mutation of $Asp^{186}$ to an alanine was assumed to prevent this amino acid from accepting a proton from the ligand, while the mutation of $Thr^{190}$ to an Ala was assumed to prevent proton donation towards the histamine heterocycle. The mutation of both amino acids would then lead to a complete loss of receptor activation (measured as cAMP response). However, these expectations are not fully confirmed by the findings of Gantz and co-workers [2]: the mutation of the aspartic acid $Asp^{186}$ to $Ala^{186}$ or $Asn^{186}$ by itself or in conjunction with the mutation of $Thr^{190}$ to $Ala^{190}$ or $Cys^{190}$ results in the loss of [methyl-$^3$H]tiotidine – a histamine $H_2$ antagonist – binding, although the generation of cAMP in response to histamine is partially maintained. The histamine $H_2$ receptor with only a $Thr^{190}$ to $Ala^{190}$ or $Cys^{190}$ mutation also retains a significant cAMP response on stimulation by histamine. Only when the negative charge of $Asp^{98}$ (from the third transmembrane domain) is removed by a mutation to $Asn^{98}$ is the receptor response to histamine totally lost [2]. Binding of the positively charged side chain of histamine to a negative receptor location, possibly followed by neutralization, appears to be essential for the activation process.

Recently, we concluded that for a series of various histamine $H_2$ receptor agonists the catalytic triad as found in serine proteases serves as a good model for studying agonistic effects on the histamine $H_2$ receptor [3,4]. This conclusion was based on molecular electrostatic potential (MEP) values, protonation energies, and $pK_a$'s for a series of imidazole- and thiazole-containing histamine $H_2$ agonists, dimaprit, and one ligand containing a selenazole ring system. A consequence of this model is that histamine binds in its proximal form. Furthermore, all known histamine $H_2$ agonists have in common that they can accept a proton in their tele-ring position with regard to the side chain [3].

This latter model [3,4] differs in two ways from the one derived before by Weinstein et al. [1, and references cited therein]: (i) a *double* proton shift at the agonistic heterocycle is not a prerequisite for receptor stimulation; and (ii) a proton is donated from the receptor towards the agonist in the tele-position and not in the proximal position, leading to a close resemblance with the catalytic triad found in serine proteases (cf. Fig. 2). Further support for our serine protease model is given by Nagy et al. [5], who calculated tautomeric and conformational equilibria of histamine both in the gas phase and aqueous solution. Under physiological conditions at pH 7.4, the equilibrium mixture was calculated to contain 64% monocation with an intramolecular hydrogen bond (i.e. the conformation with the protonated amine side-chain group coupling to the alkaline proximal ring nitrogen, and with histamine thus necessarily in its tele-tautomeric form) and 34% monocation in the proximal tautomeric form with an extended side chain [5]. We have predicted the latter conformation to be the biologically active species for the histamine $H_2$ receptor [3,4]; cf. Fig. 2. Hence, the hypothesis of histamine binding in its proximal tautomer is in agreement with the calculations of Nagy and co-workers, since a substantial amount of histamine occurs in the presumed (histamine $H_2$) biologically active conformation. In this context it is worth pointing out that the extended tele-conformation, the biologically active species in Weinstein's model (Fig. 1), appears for only 2% in the molecular partition function [5]. Furthermore, Nagy et al. [5] also point to the possibility of a subsequent activation step involving a proton donation from the receptor towards the agonist in the tele-ring position. These authors [5] conclude that all thermodynamical requirements implicit in our activation model for the histamine $H_2$ receptor (cf. Fig. 2) match the calculated equilibrium mixture of histamine in aqueous solution at physiological pH.

Using the catalytic triad of serine proteases as a model for the histamine $H_2$ receptor binding site also implies

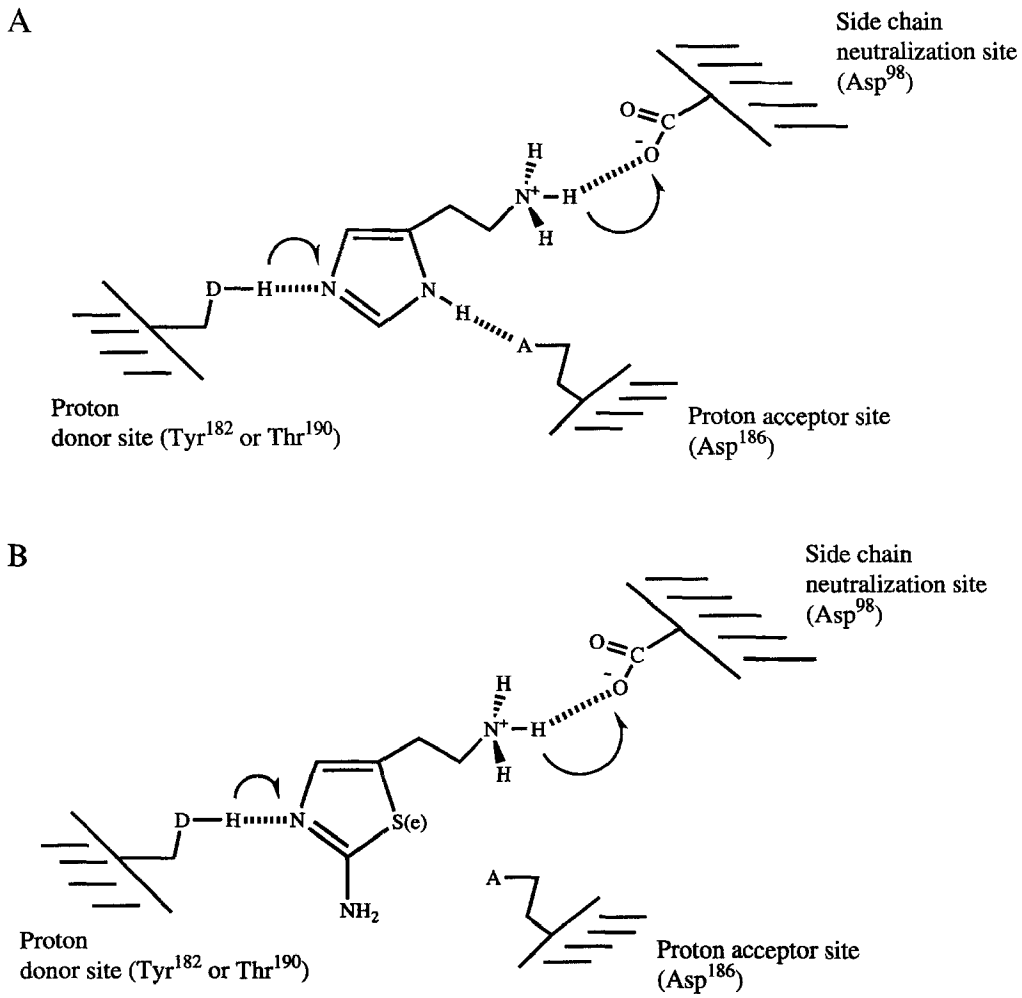


Fig. 2. The catalytic triad of serine proteases as a model for the histamine $H_2$ agonistic binding site [3]; histamine binds in its proximal tautomeric form. As a consequence, the proton-accepting and -donating groups interacting with the heterocycle are interchanged with respect to Fig. 1. Both histamine (A) and a thiazole- (or selenazole-)containing agonist (B) can accept a proton from the receptor in their tele-position. The receptor activation mechanism is considered to be initiated by a proton transfer from the receptor to the heterocycle of the agonist, thereby possibly triggering a second proton transfer from the side chain towards $Asp^{98}$ [3,4]. Arrows denote these proton movements.

that the aspartic acid from the fifth α-helix only functions as a stabilization factor which facilitates the essential step: the protonation of the agonist in the tele-position by the histamine $H_2$ receptor [3,4], which resembles the protonation of the histidine (by a serine residue) in serine proteases [6,7]. Within this model, it can well be explained why the biological response is partially (35%) maintained when $Asp^{186}$ is mutated to $Ala^{186}$ [2]. This mutation results in a less efficient proton donation from the receptor towards the agonist, but does not completely inhibit this proton transfer. Gantz et al. [2] concluded that although $Asp^{186}$ is of crucial importance in the binding of selective histamine $H_2$ antagonists, such as tiotidine, it is however not an essential element in histamine binding. As the densities of several mutants are not reported by Gantz et al. [2], it is impossible to make a thorough quantitative comparison of percentages of activation and $EC_{50}$ values between the different mutants and the wild-type receptor. However, qualitatively these experiments are very useful.

*Is there an alternative for the alleged $Asp^{186}/Thr^{190}$ binding site?*

The observation that the $Thr^{190}$ to $Ala^{190}$ mutant retains the ability to generate cAMP up to a 50% level [2] seemingly contradicts Nagy's and our earlier expectations of an essential proton transfer step from the receptor towards the agonist in the tele-position of the heterocyclic ring system [3–5]. Therefore, we searched for another amino acid with proton donor functionality in the proximity of $Asp^{186}$ at the fifth transmembrane α-helix. $Tyr^{182}$ could serve as such. From the amino acid sequence of both the human and canine histamine $H_2$ receptor [8] (which are almost identical in their membrane-bound domains), it is inferred that $Tyr^{182}$ lies one α-helical turn above $Asp^{186}$ towards the extracellular surface, whereas $Thr^{190}$ is positioned one turn below. This tyrosine residue is not only at a position closer to the extracellular surface of the receptor than $Thr^{190}$, but tyrosine is (in general) also a better proton donor than a threonine. This can be inferred from the $pK_a$ values of their side chains, i.e. 10.13 for a tyrosine in an aqueous environment, and ~13 for a hydroxyl group in a serine or threonine under similar conditions [9]. Of course, one has to bear in mind that $pK_a$ shifts can occur when the amino acids are placed in a protein environment [10].

Arguments against a possible role for $Tyr^{182}$ in binding and subsequent activation could be based on the observation that the $Thr^{190}$ to $Ala^{190}$ (or $Cys^{190}$) mutant does display impaired cAMP production and histamine binding (i.e. higher $EC_{50}$ values) compared to the wild-type receptor [2], and therefore must be involved in both binding and activation processes. However, receptors in which $Thr^{190}$ is mutated are seen to generate a higher, or at least an equal, level of cAMP compared to receptors which lack an aspartate at position 186 [2]. Although receptor densities for the 98 and 186 mutants are not given in Ref. 2, the indicated higher cAMP levels for the 190 mutants compared to the 186 mutants may very well imply that $Thr^{190}$ is less important than $Asp^{186}$ in receptor activation. Furthermore, the combined mutation, $Asp^{186}$ to $Ala^{186}$ and $Thr^{190}$ to $Ala^{190}$, does not further enhance the observed $EC_{50}$ value relative to the $Ala^{190}$ mutant, but, in contrast, a decreased $EC_{50}$ value is found [2]. This is not understood within the $Asp^{186}/Thr^{190}$ binding model, where both $Asp^{186}$ and $Thr^{190}$ are involved in histamine binding as suggested by Gantz et al. [2]. Additionally, a $Thr^{190}$ to $Cys^{190}$ mutant does not reveal a decreased $EC_{50}$ value compared to the wild type as expected for a thiol-containing residue with a significantly lower $pK_a$ value than the threonine's hydroxyl group; in contrast, the $EC_{50}$ value for the $Cys^{190}$ mutant increases. Based on the aforementioned considerations, we conclude that $Thr^{190}$ could have an indirect role in histamine binding and receptor activation rather than a direct one. Our study aims at investigating the possibilities for histamine binding to the couples $Tyr^{182}/Asp^{186}$ and $Asp^{186}/Thr^{190}$, respectively.

## Methods

*Overall strategy to approach histamine binding to its binding site at the fifth transmembrane α-helix*

In order to investigate histamine binding to the agonistic binding site at the fifth transmembrane α-helix of the histamine $H_2$ receptor, we applied the strategy depicted as a flow chart in Fig. 3. The investigations have been separated into two parts, represented by Sections I and II, which in turn consist of several steps. Section II represents histamine binding in 3D models of the transmembrane part of the histamine $H_2$ receptor and will be outlined in Part II of this study. Histamine binding to small-molecule systems is addressed here (Part I).

Due to the limitations of a complete protein model (see Part II) and to achieve computational efficiency, a rather simple model system (mini-receptor) consisting of an oligopeptide in an α-helical conformation was chosen to compare histamine binding to the respective couples Tyr/Asp and Asp/Thr (Fig. 3, step **1**, construction of the model system). Subsequently (step **2**), all possible conformations of the oligopeptide complexed with histamine were generated, and each conformation was geometry-optimized in step **3**. Since the system investigated in steps **2** and **3** of Fig. 3 consists of a supermolecule, i.e. an oligopeptide complexed with a histamine fragment, which contains several conjugated π-systems and in which intermolecular (hydrogen-bonded) interactions are of crucial importance, molecular mechanics methods were thought to be less adequate for a thorough final analysis of the data. Moreover, since the intermolecular H-bonds were biased with the aid of restraint forces and the 'minimal'

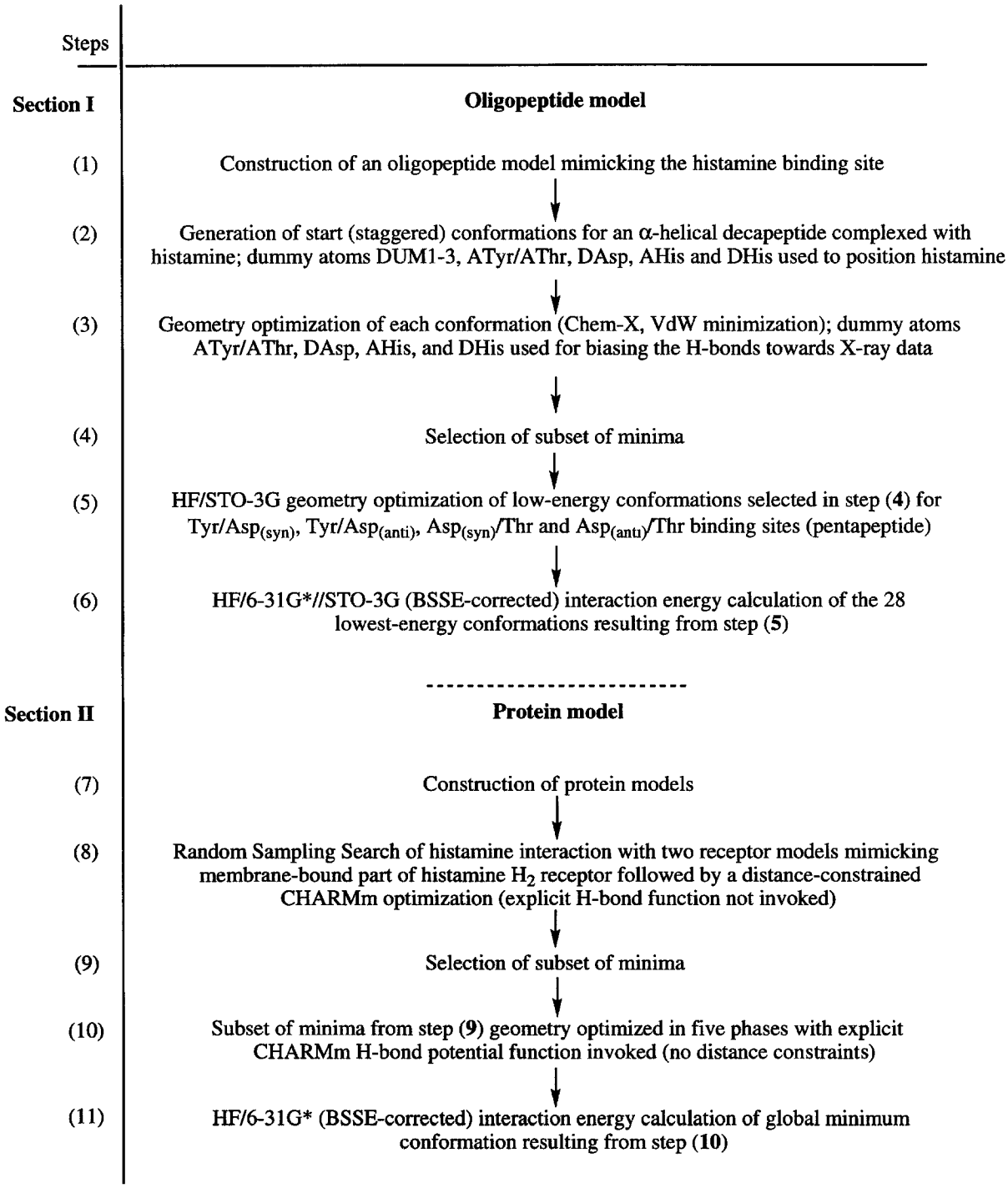


Fig. 3. Flow chart of the overall strategy to approach histamine binding to its agonistic binding site at TM5 of the histamine $H_2$ receptor. Section I: modelling histamine binding to an oligopeptide; Section II: modelling histamine binding in receptor models. Steps **1**–**6** are dealt with in this study (Part I).

vdW force field [11] was used in the molecular mechanics calculations (vide infra), validation of the results with more accurate methods is necessary. Therefore, a subset of optimized geometries for the Tyr/Asp and Asp/Thr interaction was selected (Fig. 3, step **4**) for further ab initio analysis (Fig. 3, step **5**). Finally, interaction energies were calculated (step **6**).

*A simple model system (Fig. 3, Section I)*

*Construction of a simple model system (Fig. 3, step 1)*

An oligopeptide in an α-helical conformation was built with the φ/ψ torsion angles set to the standard α-helical values (being −57° and −47°, respectively [12]; Fig. 3, step **1**). This peptide, mimicking part of the putative agonistic binding site at the histamine $H_2$ receptor, consists of 10

amino acids present in the fifth transmembrane helix (both human and canine). This decapeptide starts at $Tyr^{182}$ and ends with $Phe^{191}$ (Fig. 4). In order for $Tyr^{182}$ to be able to interact with histamine, it is necessary that this residue points into the central cavity. The following paragraph indicates this to be possible.

The histamine $H_2$ receptor is a G-protein-coupled receptor (GPCR) and possesses seven tentative transmembrane α-helices (denoted by TM1–TM7). From an analysis of a multisequence alignment of 225 GPCRs belonging to the rhodopsin superfamily, Oliveira et al. [13] assign residues which most likely point into the central cavity.

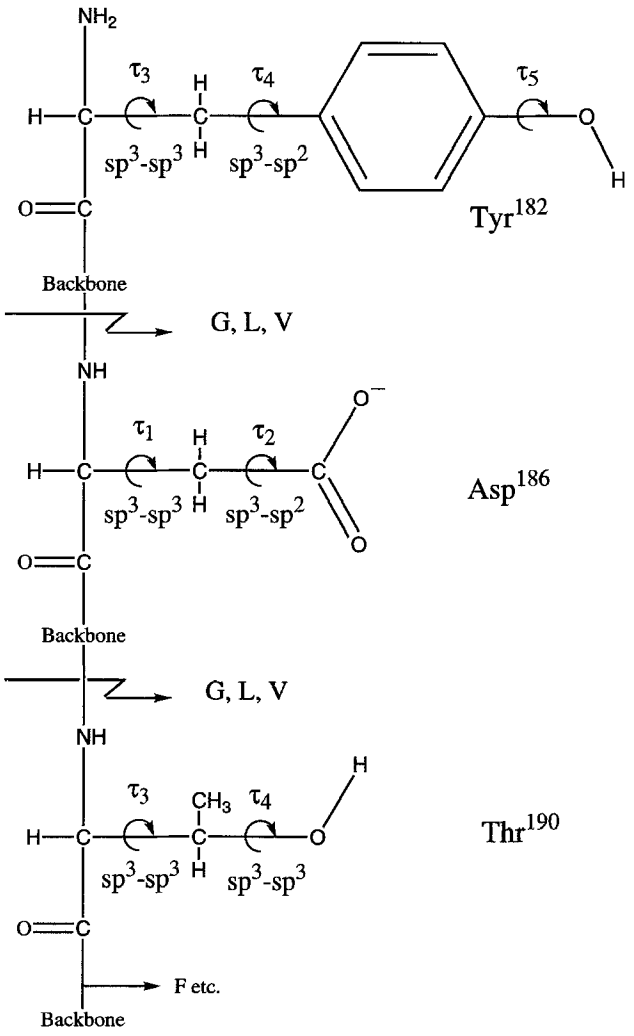


Fig. 4. Draft of the oligopeptide mimicking part of the histamine $H_2$ receptor's fifth α-helix. The torsion angles ($\tau_1$–$\tau_5$) which were allowed to vary in both molecular mechanics and ab initio calculations are depicted. The torsion angles belonging to Asp are denoted by $\tau_1$ and $\tau_2$ and are given as $C_{(backbone)}$-$C^{\alpha}$-$C^{\beta}$-$C^{\gamma}$ ($sp^3$-$sp^3$) and $C^{\alpha}$-$C^{\beta}$-$C^{\gamma}$-$O^{\delta}$ ($sp^3$-$sp^2$), respectively. The torsion angles for Thr are denoted by $\tau_3$ and $\tau_4$, and equal $C_{(backbone)}$-$C^{\alpha}$-$C^{\beta}$-$O^{\gamma}$ ($sp^3$-$sp^3$) and $C^{\alpha}$-$C^{\beta}$-$O^{\gamma}$-H ($sp^3$-$sp^3$), respectively. Finally, three torsion angles were considered for Tyr, denoted by $\tau_3$–$\tau_5$ and defined by $C_{(backbone)}$-$C^{\alpha}$-$C^{\beta}$-$C^{\gamma}$ ($sp^3$-$sp^3$), $C^{\alpha}$-$C^{\beta}$-$C^{\gamma}$-$C^{\delta}$ ($sp^3$-$sp^2$) and $C^{\delta}$-$C^{\varepsilon}$-$O^{\zeta}$-H ($sp^2$-$sp^2$), respectively. The C-O-H valence angles of $Tyr^{182}$ and $Thr^{190}$ were only optimized in the ab initio calculations.

The residues in the $Tyr^{182}$-$Phe^{191}$ sequence which point with their side chain into the central cavity are denoted with a 'o': YG°LVD°G°LVT°F; these are $Gly^{183}$, $Asp^{186}$, $Gly^{187}$ and $Thr^{190}$ [13]. In an α-helix, a 360° turn is spanned by 3.6 amino acids (a 100° turn per amino acid). Since Gly allows more freedom in the $\phi/\psi$ angles than any other amino acid (and hence introduces special entropy effects [14,15]), and because of the presence of even two glycines (at positions 183 and 187) in the $Tyr^{182}$-$Phe^{191}$ sequence [8], it is not unlikely that $Tyr^{182}$ also points towards the central cavity in the $H_2$ receptor. The presence of these two Gly residues appears to be specific for the histamine $H_2$ receptor (e.g. Ref. 13, and references cited therein). Hence, $Tyr^{182}$ not only has a reasonable $pK_a$ to be able to donate a proton from the receptor towards the agonist but could additionally point into the central cavity. The enhanced flexibility of the backbone, due to the presence of Gly residues in TM5, will be addressed in more detail in Part II of this study. Within this first part, imidazole binding to a pure α-helical oligopeptide is considered and therefore the backbone was kept fixed at standard α-helical torsion angles.

The oligopeptide was not taken in its zwitterionic state because in the histamine $H_2$ receptor both $Tyr^{182}$ and $Phe^{191}$ are involved in peptide bonds and are thus not charged. The zwitterionic state of the decapeptide would introduce additional nonrealistic electrostatic interactions between the α-helix and the histamine fragment in subsequent geometry optimizations. Since the side chain of histamine has been proven to interact with $Asp^{98}$ [2] from TM3, we have chosen for a neutral side chain throughout the calculations, again in order to prevent unrealistic ionic interactions between the oligopeptide mimicking the fifth transmembrane α-helix and the histamine side-chain amino group. The initial geometry for histamine was taken from X-ray data [16].

*Generation of start points and positioning of the histamine fragment relative to the oligopeptide (Fig. 3, step 2)* Within the $Tyr^{182}$-$Phe^{191}$ α-helical oligopeptide, two possible sites for interaction with the histamine imidazole ring system were investigated: (a) the $Tyr^{182}$/$Asp^{186}$ couple; and (b) the $Asp^{186}$/$Thr^{190}$ couple.

The complete conformational space accessible to the amino acids constituting the two binding sites was explored by considering all possible staggered orientations in the side chains under investigation as start points. An $sp^3$-$sp^3$ bond results in three staggered low-energy conformations (see the Newman projections in Fig. 5), whereas an $sp^3$-$sp^2$ bond yields six low-energy staggered conformations (Fig. 5). Based on these low-energy staggered conformations, 324 local minima were generated for the Tyr/Asp couple (a), since both Tyr and Asp contain one $sp^3$-$sp^3$ and one $sp^3$-$sp^2$ bond. The Tyr C-C-O-H torsion angle was fixed in the plane due to the alleged $sp^2$-like character of the phenolic oxygen atom [17]. For the Asp/

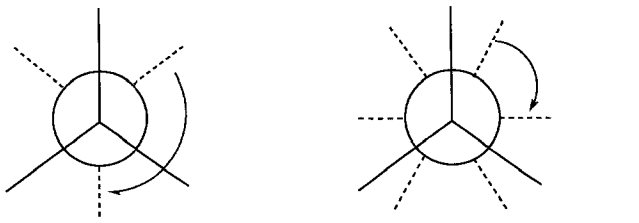

$sp^3$-$sp^3$: 3 local minima (60°-180°-300°)

$sp^3$-$sp^2$: 6 local minima (30°- 90°-150°-210°-270°-330°)

($\tau_1$; $\tau_3$; $\tau_4$ in $Asp^{186}$/$Thr^{190}$)

($\tau_2$; $\tau_4$ in $Tyr^{182}$/$Asp^{186}$, cf. Fig.4)

Fig. 5. Staggered conformations for $sp^3$-$sp^3$ and $sp^3$-$sp^2$ bonds depicted as Newman projections.

Thr couple (b), 162 minima were generated since Thr possesses two $sp^3$-$sp^3$ bonds. The possibility of either a syn- or an anti-orientated binding to the carboxylate doubles the number of low-energy conformations to be investigated (i.e. 648 for the Tyr/Asp interaction and 324 for the Asp/Thr couple). Indeed, Ippolito et al. [17] have shown that H-bonds between a histidine imidazole ring and a carboxylate group occur for 63.2% in the syn orientation and for 36.8% in the anti orientation (vide infra).

For each staggered start position generated in the conformational analysis on the two couples (a) and (b), histamine (in its proximal tautomeric form) was positioned in between the functional groups found in the amino acid side chains. For this purpose, dummy atoms were introduced on both the oligopeptide and histamine. Three dummies were used to position the histamine side chain towards the proposed central cavity (Fig. 3, step **2**), whereas six dummies were introduced to bias hydrogen bond geometries towards X-ray data (Fig. 3, step **3**) and to position the imidazole ring relative to the respective binding sites (Fig. 3, step **2**). The following paragraph discusses the function of the first three dummies, whereas the latter six are discussed in subsequent paragraphs.

Since histamine is not only known to interact with TM5 but also interacts via its side chain with TM3, this side chain should point towards the protein interior [13]. The side-chain amino group is likely to be neutralized at $Asp^{98}$ from TM3 [1,2]. In order to direct the side chain into the direction of the central cavity while histamine simultaneously interacts with the $Tyr^{182}$-$Phe^{191}$ oligopeptide, three dummy atoms were introduced. These three dummy atoms were positioned at a distance of 10 Å from the $C^{\alpha}$ atom of $Tyr^{182}$, $Asp^{186}$ and $Thr^{190}$, respectively, and in a direction defined by the corresponding $C^{\alpha}$-$C^{\beta}$ vector (DUM1, DUM2 and DUM3 in Fig. 6). Since both $Asp^{186}$ and $Thr^{190}$ are thought to point into the central cavity [13], their $C^{\alpha}$-$C^{\beta}$ bonds will also point towards the receptor interior. For investigating the binding of histamine to the Asp/Thr binding site, the amino group of the histamine side chain was fitted in between dummies DUM2 and DUM3. During this fit, the geometry of both histamine and the oligopeptide was kept fixed, which is called rigid fitting and gives the best initial orientation of histamine within the complex. A rigid fit is defined in terms of atoms to be superimposed, and relatively higher restraint constants (weighting) are specified for those pairs of atoms which have to fit more closely than others. The amino group of the side chain was specified to match

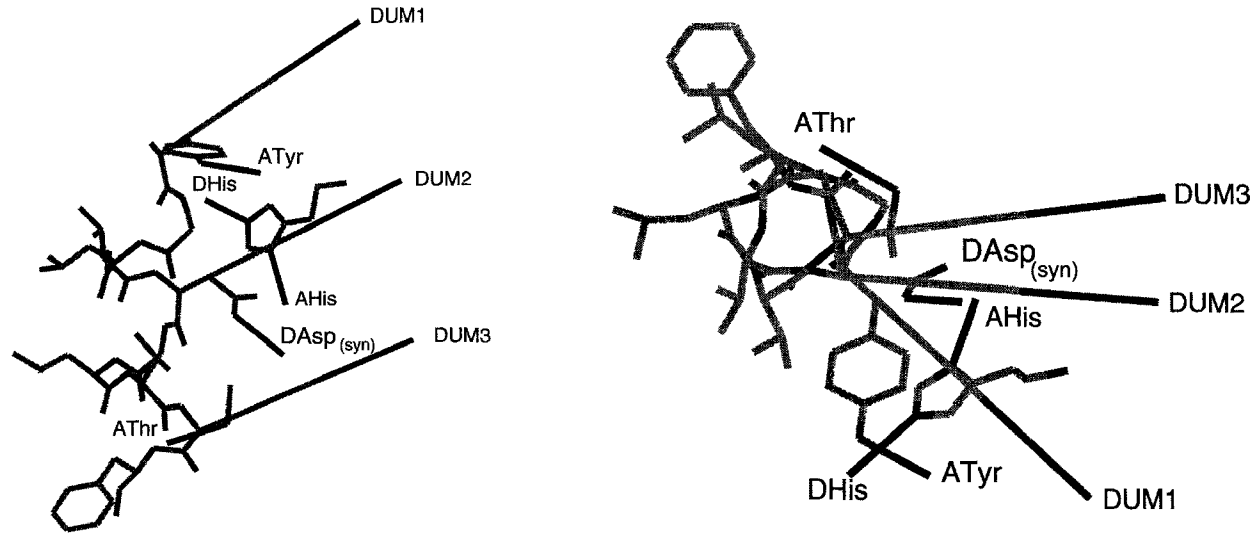


Fig. 6. Draft of a decapeptide representing a part of the fifth transmembrane α-helix of the histamine $H_2$ receptor (side and top views). Histamine is positioned in between $Tyr^{182}$ and $Asp^{186}$ with the aid of dummy atoms DUM1, DUM2, ATyr, $DAsp_{(syn)}$, AHis and DHis (the situation before minimization). Here, $Thr^{190}$ in one of its (standard Newman) minima is seen to interact with the backbone via an H-bond. DAsp, ATyr and AThr are dummy atoms put at positions where an interaction with the hetero ring atoms of histamine is to be expected (for details see Fig. 7). Also the dummy atoms AHis and DHis are indicated (cf. Fig. 7). DUM1–DUM3 are dummy atoms for defining the direction of the receptor's cavity. These dummies are used to direct the side chain of histamine towards $Asp^{98}$ by fitting the side-chain nitrogen in between DUM1 and DUM2 for the Tyr/Asp couple (depicted) or in between DUM2 and DUM3 (for investigating the binding at the Asp/Thr couple; not depicted).

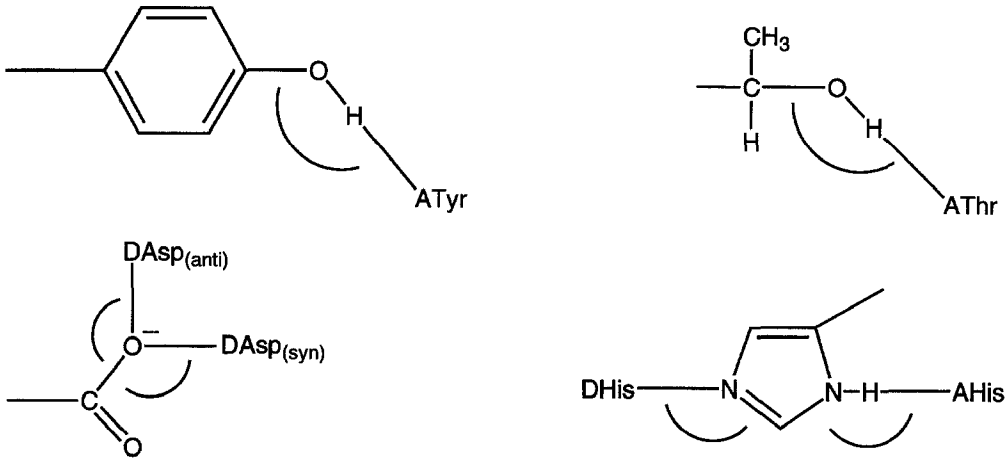


Fig. 7. Ippolito et al. [17] analysed the Brookhaven Protein Database for recurring motifs in hydrogen bond geometries. The mean X-ray values are used to position dummy atoms: ATyr at 2.9 Å (±0.3) and 119° (±14); AThr at 2.9 Å (±0.2) and 117° (±17); $DAsp_{(syn)}$ and $DAsp_{(anti)}$ at 2.9 Å (±0.2) and 120°; AHis and DHis at 3.0 Å (±0.2) and 119° (±21) (with deviations in parentheses). The dummy atoms for Tyr, Asp and His were placed within the aromatic plane, whereas AThr is positioned at a standard tetrahedral value (109°); deviations from dihedral angles are not given in Ref. 17.

with both DUM2 and DUM3 with moderate weighting factors, while for the imidazole ring system higher weighting factors were used (via dummy atoms AThr, DAsp, AHis and DHis; Figs. 6 and 7; vide infra). In this way, the imidazole heterocycle can interact with the Asp/Thr binding site with H-bond geometries as close as possible to X-ray data, while the side-chain amino group points into the central cavity. For the Tyr/Asp couple a similar fitting procedure was followed. Since TM5 and, thus, also $Gly^{183}$ and $Gly^{187}$ were built with standard $\phi/\psi$ α-helical torsion angles, the side chain of $Tyr^{182}$, and hence DUM1, will possibly not point towards the receptor's interior [13]. However, the side-chain amino group of histamine was fitted in between DUM1 and DUM2, and therefore the amino group is still expected to point into the histamine $H_2$ receptor's central cavity. Hence, for both couples, Tyr/Asp and Asp/Thr, the histamine side-chain amino group is prevented from unrealistic (and thus undesired) interactions with the oligopeptide mimicking a part of TM5 (cf. Fig. 6, where histamine is depicted within a certain staggered (Newman) geometry of the oligopeptide; the side chain is seen not to interact with the decapeptide). N.B.: DUM1–DUM3 were only regarded at step **2** of the flow chart (Fig. 3) and were removed in the subsequent geometry optimization process (Fig. 3, step **3**).

Dummies (ATyr/AThr, $DAsp_{(syn)}$, $DAsp_{(anti)}$, AHis and DHis) were positioned at hydrogen bond distances, valence angles and torsion angles as obtained by Ippolito et al. [17] from a thorough X-ray data analysis study on a protein database. Since both histamine and histidine possess an imidazole ring system, the X-ray data on the H-bonds of the histidine imidazole ring were used for histamine. The mean X-ray values which determine the positions of the dummies are depicted in Fig. 7. The dummies in Fig. 7 were put at those positions where the respective hydrogen bond donor or acceptor heteroatom is to be expected, e.g. dummy ATyr is put at a position where the presence of a hydrogen bond acceptor is expected (in casu the basic $N^{\tau}$ of the histamine imidazole ring), and DHis is at a position where a hydrogen bond donor is expected (in casu the hydroxyl O in $Tyr^{182}$ or $Thr^{190}$). Thus, in case $Tyr^{182}$ donates its hydrogen to the $N^{\tau}$ of histamine, ATyr should coincide with the position of $N^{\tau}$, whereas DHis should match with the position of the hydroxyl oxygen. In case $Thr^{190}$ functions as a proton donor towards the $N^{\tau}$, AThr should match with $N^{\tau}$, and DHis again with the hydroxyl oxygen. Two dummies were connected to $Asp^{186}$, since this residue can accept protons both in the so-called syn- and anti-positions; these are denoted by $DAsp_{(syn)}$ and $DAsp_{(anti)}$, respectively. One of these dummies should match with the proximal nitrogen (-$N^{\pi}$H-) of histamine, and AHis with one of the carboxylate's oxygens (Figs. 7 and 8). In summary, for the interaction site $Tyr^{182}/Asp^{186}$ the following matches have to be aimed at: ATyr-$N^{\tau}$; DHis-Tyr-O; AHis-Asp-O; DAsp-$N^{\pi}$. For the $Asp^{186}/Thr^{190}$ interaction site we aimed at matching AThr-$N^{\tau}$, DHis-Thr-O, AHis-Asp-O and DAsp-$N^{\pi}$ (cf. Fig. 8). The dummy atoms do not only aid in positioning the imidazole with respect to the oligopeptide, but, by enforcing penalty functions on the distances between these (dummy) atom pairs, the results of a molecular mechanics geometry optimization (Fig. 3, step **3**) can also be biased towards X-ray hydrogen bond results.

*Molecular mechanics geometry optimization (Fig. 3, step 3)* The third step in the flow chart (Fig. 3, step **3**) concerns a molecular mechanics geometry optimization on each conformation of the supermolecule consisting of the oligopeptide (with the side chains of its interacting amino acids in exact staggered positions) and the histamine fragment. For the molecular mechanics geometry

optimizations, the programme Chem-X [11] was chosen because, firstly, it allows the introduction of dummy atoms which are fitted on target atoms with user-defined restraint forces and, secondly, the large number of conformations to be analysed requires a relatively simple but fast force field. Therefore, the so-called 'minimal' vdW force field [11] was applied, which only varies selected torsion angles and fragment orientations; all bond lengths and valence angles remain fixed. The nonbonded interactions and the hydrogen bonds in the vdW procedure are given in Eqs. 1 and 2, respectively (vide infra). By introducing forces between dummy atoms and their targets (heteroatoms in Figs. 6 and 7), the results of a Chem-X molecular mechanics geometry optimization can be biased to favour X-ray-estimated hydrogen bonds (Fig. 8). In the study of either binding site, the Tyr/Asp or Asp/Thr couple, the vdW force field was expanded with four restraint forces ($F_r$, Eq. 3). For this purpose, the dummy atoms, also applied in positioning the imidazole ring system within the putative binding site, were used. There were no restraints imposed on the histamine side chain with respect to dummies DUM1–DUM3 during the vdW geometry optimization.

*H-bonds and molecular mechanics; the necessity of restraint forces* In order to describe an H-bond properly, not only the distances between the heteroatoms involved in hydrogen bonding should be considered, but also angle (both valence and torsion) preferences must be included. This is illustrated by the findings of Ippolito et al. [17] for the binding of positively charged residues (Arg, His, Lys) to carboxylate groups via salt bridges. The syn-orientation was reported to occur predominantly, with the syn-orientated hydrogen bonds found more frequently in the plane of the carboxylate and in the direction of the oxygen's lone electron pair than the anti-orientated ones. The resulting salt bridges were concluded to be electrostatically optimal for the syn-orientated hydrogen bonds to the carboxylate, and the syn-interaction was considered to have a stronger alkaline character leading to stronger interactions than the anti-orientation [17].

In Chem-X [11], electrostatic interactions are computed by the monopole–monopole term from Coulomb's law, whereas the nonbonded interactions are described by

$$E_{nb} = A \exp(-Br)/r^D - C/r^6 \quad (1)$$

where A, B, C and D are constants depending on the atom-type pair. The internuclear distance is given as r (in Å) and Eq. 1 is seen to be a mixture of the Lennard-Jones expression (B=0; D=12) and the Buckingham term (D=0). For details regarding parametrization, the reader is referred to Del Re et al. [18].

The electrostatic interaction term plays a dominant role in the overall geometry of H-bonds, provided higher order multipoles are included [19,20]. The Chem-X [11] hydrogen-bonding term equals

$$E_{hb} = (C/r^A) - (D/r^B) \quad (2)$$

Here, A and B are global integer constants, C and D are parameters for the atom-type pair, and r is the interatomic distance (Å). Because the repulsive energy between the hydrogen-bonded atoms in Eq. 2 is too high to reproduce experimental distances and energies, r is scaled automatically by a factor with a default value of 1.31 (see Ref. 11 for further details). Hence, in Chem-X [11], multipoles are omitted in the electrostatic term and hydrogen bonds are treated as non-bonded-like interactions (cf. Eqs. 1 and 2), which implies that directionality in H-bond geometries is not included: the angle dependence of H-bonds is obviously lacking. However, Ippolito et al. [17] have clearly demonstrated the angular dependence of hydrogen bonds, and in the next paragraph we present a method to extend the Chem-X force field [11] in order to address H-bonds involved in histamine binding to the receptor in a more accurate manner.

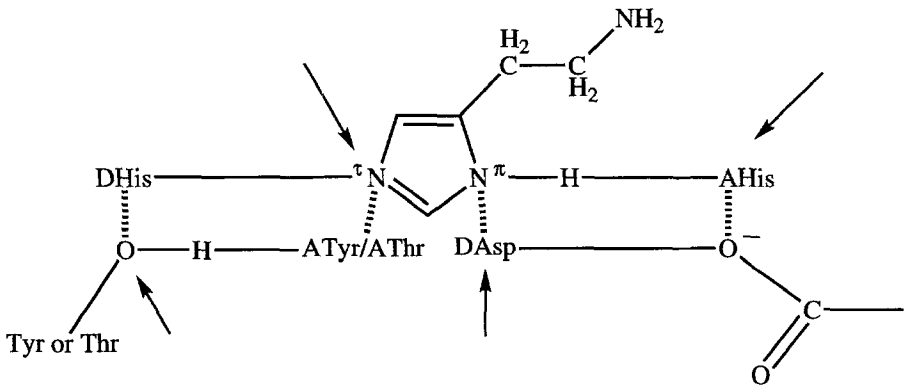


Fig. 8. In order to bias the results of a molecular mechanics geometry optimization (Fig. 3, step **3**), dummy atoms are superimposed on heteroatoms: dummies are at ideal positions for H-bond formation between an imidazole (DHis and AHis, cf. Fig. 7), a carboxylate ($DAsp_{(syn)}$ and $DAsp_{(anti)}$) and a hydroxyl in either a threonine or tyrosine (AThr and ATyr, respectively, cf. Figs. 6 and 7). (N.B.: Arrows denote the four fit points; '≡' represents an additional restraint force: k·Δr, Eq. 3.)

TABLE 1

GEOMETRICAL AND ENERGY DATA FOR 28 Chem-X [11] MINIMA, RESULTING FROM A CONFORMATIONAL SEARCH WITH SUBSEQUENT GEOMETRY OPTIMIZATION[a]

| Minimum | Syn/anti | $\tau_1$ [b] | $\tau_2$ [b] | $\tau_3$ [b] | $\tau_4$ [b] | $\tau_5$ b | $\Sigma\Delta_{dum}$ [c] | $E_{inter}$ [d] | $E_{intra}$ oligo [d] | Strain-corrected $E_{inter}$ [d] | $N^{\pi}...O_{(A)}$ [e] | $N^{\pi}-H^{\pi}...O_{(A)}$ | $N^{\pi}...O_{(A)}-C_{(A)}$ | $N^{\pi}...O_{(A)}-C_{(A)}-C_{(A)}$ | $O_{(T)}...N^{\tau}$ [f] | $O_{(T)}-H_{(T)}...N^{\tau}$ | $H_{(T)}...N^{\tau}-C_2$ |
|---|---|---|---|---|---|---|---|---|---|---|---|---|---|---|---|---|---|
| **Asp/Thr** | | | | | | | | | | | | | | | | | |
| 1 | syn | −179 | 110 | −135 | 131 | – | 3.36 | 0.28 | 12.72 | 13.00 | 2.89 | 142.4 | 120.2 | −179.1 | 2.95 | 165.9 | 111.4 |
| 2 | | 170 | −150 | −154 | 164 | – | 3.79 | −3.53 | 24.21 | 20.68 | 2.98 | 147.3 | 118.6 | 178.5 | 2.92 | 151.7 | 114.1 |
| 3 | | 176 | 126 | −137 | 139 | – | 3.38 | 8.66 | 12.31 | 20.97 | 2.91 | 144.3 | 120.0 | −178.7 | 2.95 | 163.8 | 111.6 |
| 4 | | 176 | 124 | −137 | 138 | – | 3.37 | 8.71 | 16.92 | 25.63 | 2.91 | 143.7 | 120.3 | −179.4 | 2.94 | 163.9 | 111.7 |
| 5 | | 134 | −117 | 129 | −150 | – | 3.23 | 2.14 | 66.38 | 68.52 | 2.80 | 135.1 | 121.6 | 177.5 | 2.99 | 180.0 | 108.8 |
| 6 | | 132 | −113 | 131 | −147 | – | 3.24 | 2.75 | 66.57 | 69.32 | 2.80 | 135.1 | 113.5 | 178.3 | 3.00 | 177.7 | 109.6 |
| 7 | | 133 | −114 | 129 | −149 | – | 3.22 | 5.69 | 67.37 | 73.06 | 2.80 | 134.8 | 121.6 | 178.4 | 2.99 | 178.1 | 109.1 |
| 8 | anti | −88 | −128 | 71 | −143 | – | 2.72 | −13.55 | 24.30 | 10.75 | 2.95 | 149.5 | 118.3 | −4.0 | 2.97 | 166.4 | 112.7 |
| 9 | | −63 | −96 | −100 | 104 | – | 0.86 | −36.38 | 56.13 | 19.75 | 3.10 | 173.0 | 120.8 | 0.9 | 3.03 | 177.5 | 121.6 |
| 10 | | −66 | −128 | −68 | 139 | – | 2.42 | −32.91 | 62.84 | 29.93 | 2.97 | 155.3 | 116.7 | −3.7 | 2.95 | 165.6 | 114.7 |
| 11 | | −90 | −128 | 73 | −145 | – | 2.72 | 12.07 | 22.51 | 34.58 | 2.79 | 163.8 | 111.9 | 5.3 | 2.98 | 167.5 | 105.4 |
| 12 | | −63 | −96 | −101 | 106 | – | 0.89 | −18.40 | 84.26 | 65.86 | 3.10 | 173.0 | 120.9 | −0.8 | 3.04 | 177.1 | 121.6 |
| 13 | | −61 | −98 | −95 | 106 | – | 0.89 | −1.47 | 80.73 | 79.26 | 3.07 | 170.7 | 120.4 | −0.7 | 3.02 | 176.1 | 120.9 |
| 14 | | −64 | −100 | −101 | 109 | – | 0.89 | 1.01 | 99.26 | 100.27 | 3.10 | 172.6 | 121.0 | −0.4 | 3.04 | 177.6 | 121.3 |
| **Tyr/Asp** | | | | | | | | | | | | | | | | | |
| 15 | syn | −73 | −36 | −131 | 154 | 111 | 3.58 | −35.85 | 31.11 | −4.74 | 3.10 | 159.7 | 128.4 | 175.5 | 2.87 | 141.5 | 118.9 |
| 16 | | 123 | −81 | 88 | 80 | −44 | 5.02 | −34.61 | 60.96 | 26.35 | 2.74 | 129.1 | 112.3 | 157.4 | 3.20 | 173.8 | 112.9 |
| 17 | | 112 | 109 | 88 | −93 | 132 | 4.65 | −28.40 | 38.19 | 9.79 | 2.61 | 120.2 | 114.7 | −159.7 | 3.19 | 172.0 | 111.4 |
| 18 | | −57 | −72 | −129 | 156 | 103 | 3.82 | −2.51 | 29.65 | 27.14 | 3.10 | 163.2 | 135.2 | 175.9 | 2.75 | 133.9 | 119.9 |
| 19 | | −76 | −54 | −137 | 156 | 107 | 3.48 | −13.66 | 70.39 | 56.73 | 3.03 | 155.5 | 126.2 | 173.5 | 2.84 | 148.0 | 116.4 |
| 20 | | −77 | −70 | −140 | 165 | 94 | 3.45 | −22.05 | 84.33 | 62.28 | 3.01 | 153.3 | 124.4 | 174.1 | 2.86 | 149.4 | 115.2 |
| 21 | | −84 | −69 | −144 | −124 | −154 | 3.54 | 19.14 | 78.21 | 97.35 | 2.95 | 147.9 | 123.8 | 173.5 | 2.93 | 155.0 | 113.7 |
| 22 | anti | 175 | 86 | −156 | −175 | 106 | 1.91 | −36.45 | 37.49 | 1.04 | 3.13 | 169.1 | 123.3 | −1.9 | 2.94 | 159.3 | 121.3 |
| 23 | | 169 | 89 | −160 | 70 | −140 | 1.86 | 6.10 | 2.95 | 9.05 | 3.09 | 166.1 | 122.5 | −2.4 | 2.97 | 162.3 | 120.3 |
| 24 | | 174 | 87 | −157 | 7 | −77 | 1.86 | −27.79 | 37.70 | 9.91 | 3.11 | 169.6 | 122.5 | −2.1 | 2.95 | 158.9 | 121.5 |
| 25 | | 171 | 87 | −158 | −169 | 100 | 1.88 | −9.05 | 22.19 | 13.14 | 3.10 | 165.8 | 123.2 | −2.7 | 2.96 | 161.2 | 121.4 |
| 26 | | 166 | 93 | −160 | 64 | −136 | 1.84 | 16.91 | 2.72 | 19.63 | 3.09 | 167.0 | 122.1 | −2.9 | 2.97 | 162.6 | 119.9 |
| 27 | | 159 | 103 | −164 | 78 | −154 | 1.79 | 32.56 | 34.97 | 67.53 | 2.98 | 165.0 | 123.5 | −3.6 | 2.98 | 162.9 | 118.8 |
| 28 | | 163 | 101 | −162 | 64 | −143 | 1.74 | 33.77 | 35.57 | 69.34 | 3.02 | 168.7 | 123.0 | −2.3 | 2.94 | 160.8 | 120.2 |

[a] All distances in Å, angles in ° and energies in kcal/mol.

[b] See Fig. 4 for the definition of $\tau_1$–$\tau_5$.

[c] Sum over the distances between the dummies and their respective target heteroatoms (see the 'Overall strategy' section and Figs. 7 and 8 for details).

[d] $E_{inter}$, total energy of the complex minus the intramolecular energies of the separate entities (histamine and oligopeptide); $E_{intra}$ oligo, energy of the oligopeptide relative to its global minimum (cf. Table 2), this value is regarded as the strain energy imposed by the ligand on the peptide; strain-corrected $E_{inter}$ calculated as $E_{inter}$ minus $E_{intra}$ oligo. (N.B.: The strain in histamine is not considered.)

[e] Subscript (A) denotes $Asp^{186}$.

[f] Subscript (T) denotes $Tyr^{182}$ or $Thr^{190}$.

TABLE 2
GLOBAL MINIMA OF THE OLIGOPEPTIDE OBTAINED FROM MOLECULAR MECHANICS (Chem-X) EVALUATIONS

| Couple | $\tau_1$ [a] | $\tau_2$ [a] | $\tau_3$ [a] | $\tau_4$ [a] | $\tau_5$ [a] | $E_{intra}$ oligo [b] |
|---|---|---|---|---|---|---|
| Asp/Thr | −70 | −117 | 41 | −132 | – | 0.00 |
| Tyr/Asp | 166 | 93 | −160 | 73 | −146 | 0.00 |

[a] See Fig. 4 for the definition of $\tau_1$–$\tau_5$.
[b] The intramolecular energy of the oligopeptide in its global minimum is set to 0.0 kcal/mol; the intramolecular energy values of the structures in Table 1 are given relative to either of these two global minima. The intramolecular energy can therefore be seen as the strain energy imposed on the oligopeptide by histamine binding: $E_{intra}$ oligo = $E_{strain}$.

The dummy atoms placed at the side chains of $Tyr^{182}$, $Asp^{186}$ and $Thr^{190}$ and at the histamine imidazole group were not only used for positioning histamine in its putative binding site, but also for biasing the molecular mechanics force field towards H-bond geometries in agreement with X-ray data. The lack of the angle dependence in Chem-X [11] can partially be overcome by extending the standard molecular mechanics force field with so-called (harmonic) restraint forces:

$$F_r = k \cdot \Delta r \qquad (3)$$

with k the restraint force constant (with a recommended value of 100) and Δr the distance between the two atoms to be superimposed, i.e. the dummy atom and the respective heteroatom assumed to coincide (Fig. 8). The forces represent penalty functions: although there are no energy terms added to the total molecular mechanics energy function (i.e. the total energy is not directly affected), the restraint forces alter the force field, thereby creating a different final geometry.

An advantage of using restraint forces, with a (recommended) value of 100 [11], is that they are high enough to allow for passing rotational barriers, provided there are no serious steric hindrances. Thus, starting within a specific staggered (Newman) conformation, the optimization can end up close to another staggered geometry in which the hydrogen bonds are best achieved (Fig. 8).

*Technical details of the molecular mechanics geometry optimization* Each (Newman) start geometry obtained in step **2** (Fig. 3) was optimized with the vdW geometry optimization procedure [11]. In the vdW optimizations, *only* the position of the rigid X-ray structure of histamine [16] was optimized with respect to the oligopeptide and those dihedral angles which could be important for histamine binding (Fig. 4, $\tau_1$–$\tau_5$). For every optimized geometry, the vdW energy values of the total complex (i.e. the histamine fragment with the peptide) and of the separate fragments (i.e. (rigid) histamine and the oligopeptide) were determined. From these data the interaction energy ($E_{inter}$, Table 1) can be obtained, being the energy of the total complex minus the intramolecular energies of histamine and the oligopeptide. Also the global minimum for each binding site (Tyr/Asp and Asp/Thr) was established in the absence of histamine and in the absence of the dummy atoms (and thus without restraint forces; Table 2). When the intramolecular energy values of the oligopeptide fragments are taken relative to these global minima values, strain energies, imposed by the ligand binding, are obtained ($E_{intra}$ oligo, Table 1). Strain-corrected interaction energies (strain-corrected $E_{inter}$, Table 1) for histamine with the oligopeptide are then calculated by subtracting the strain energy ($E_{intra}$ oligo) from the interaction energy ($E_{inter}$). Finally, the deviations from the desired (mean) X-ray hydrogen bond values were calculated, i.e. a sum over all deviations between the positions of the dummy atoms and their target heteroatoms ($\Sigma\Delta_{dum}$; cf. Fig. 6 and Table 1). A subset of molecular mechanics optimized geometries was selected for each couple (a) and (b) for subsequent ab initio calculations.

*Selection of a subset of local minima (Fig. 3, step 4)* Seven conformations for each syn- and anti-orientated Tyr/Asp and Asp/Thr interaction were selected (Fig. 3, step **4**) for further ab initio analysis (Fig. 3, step **5**). This selection was based on both energy and geometry data obtained from the molecular mechanics geometry optimization procedure. Considering the total energy of the complex, the four lowest energy geometries were selected for each couple Tyr/Asp and Asp/Thr (both syn and anti). Three further conformations were selected on the basis of

TABLE 3
HF/6-31G*//STO-3G VALUES FOR THE GLOBAL MINIMA OF THE OLIGOPEPTIDE UNDER CONSIDERATION[a]

| Couple | $\tau_1$ [b] | $\tau_2$ [b] | $\tau_3$ [b] | $\tau_4$ [b] | $\tau_5$ [b] | $E_{intra}$ oligo [c] |
|---|---|---|---|---|---|---|
| Asp/Thr | −61.1 | −170.3 | 54.7 | −78.1 | – | −1489.0733 |
| Tyr/Asp | −89.5 | −162.1 | 173.9 | 81.5 | −115.8 | −1679.5650 |

[a] The molecular mechanics global minima from Table 2 were used as initial structures for the HF/STO-3G geometry optimizations.
[b] See Fig. 4 for the definition of $\tau_1$–$\tau_5$.
[c] In atomic units (au).

TABLE 4
HF/6-31G*//STO-3G RESULTS

| Minimum | Syn/ anti | $\tau_1$ [a] | $\tau_2$ [a] | $\tau_3$ [a] | $\tau_4$ [a] | $\tau_5$ [a] | $N^{\pi}...O_{(A)}$ [b] | $N^{\pi}$-$H^{\pi}...O_{(A)}$ | $N^{\pi}...O_{(A)}$-$C_{(A)}$ | $N^{\pi}...O_{(A)}$-$C_{(A)}$-$C_{(A)}$ | $O_{(T)}...N\tau$ [c] | $O_{(T)}$-$H_{(T)}...N^{\tau}$ |
|---|---|---|---|---|---|---|---|---|---|---|---|---|
| **Asp/Thr** | | | | | | | | | | | | |
| 1 | syn | 170.7 | 96.7 | −151.1 | 149.7 | – | 2.39 | 172.9 | 110.8 | −159.3 | 2.90 | 155.6 |
| 2 | | −175.4 | −126.5 | −152.9 | 157.1 | – | 2.38 | 172.0 | 116.0 | 153.5 | 2.92 | 159.1 |
| 3 | | 170.4 | 97.1 | −151.1 | 151.5 | – | 2.40 | 172.8 | 110.7 | −159.8 | 2.91 | 155.3 |
| 4 | | 171.0 | 94.6 | −150.8 | 150.8 | – | 2.40 | 172.9 | 110.9 | −160.0 | 2.91 | 155.7 |
| 5 | | −161.3 | −81.4 | 54.0 | −87.0 | – | 2.41 | 176.7 | 115.4 | −177.6 | 5.87 | 102.1 |
| 6 | | 70.6 | −32.9 | 57.9 | −171.8 | – | 2.40 | 178.2 | 114.3 | −169.4 | 8.46 | 118.0 |
| 7 | | 170.0 | −74.4 | 54.7 | −156.5 | – | 2.39 | 178.8 | 115.3 | −171.6 | 4.74 | 149.2 |
| 8 | anti | −79.9 | −132.5 | 46.4 | −162.0 | – | 2.38 | 172.2 | 117.6 | 21.4 | 2.85 | 163.0 |
| 9 | | −59.4 | −153.4 | −47.9 | 61.5 | – | 2.41 | 176.1 | 120.0 | 62.1 | 5.82 | 102.8 |
| 10 | | −82.5 | −127.6 | −49.4 | 168.3 | – | 2.40 | 176.5 | 118.8 | 17.4 | 2.75 | 152.7 |
| 11 | | −98.9 | −132.5 | 47.0 | −163.4 | – | 2.38 | 173.3 | 117.8 | 21.6 | 2.85 | 162.0 |
| 12 | | −55.9 | −172.6 | −46.9 | 64.9 | – | 2.40 | 177.7 | 122.2 | −11.4 | 7.12 | 98.6 |
| 13 | | −60.8 | −153.1 | −42.8 | 62.9 | – | 2.42 | 177.8 | 120.2 | 76.4 | 6.36 | 102.4 |
| 14 | | −71.5 | −122.9 | −72.4 | 93.1 | – | 2.39 | 174.4 | 116.4 | 26.9 | 2.77 | 147.6 |
| **Tyr/Asp** | | | | | | | | | | | | |
| 15 | syn | −64.2 | −63.6 | −139.0 | 141.9 | 137.4 | 2.37 | 173.8 | 120.2 | 153.4 | 2.73 | 165.8 |
| 16 | | 157.9 | 129.4 | 89.2 | −79.9 | 167.4 | 2.38 | 176.2 | 116.1 | 81.1 | 2.70 | 173.7 |
| 17 | | −164.3 | −130.8 | 84.9 | 101.8 | −19.6 | 2.37 | 175.7 | 123.0 | −62.5 | 2.68 | 172.2 |
| 18 | | −65.0 | −60.4 | −146.3 | 98.0 | 174.3 | 2.38 | 174.8 | 125.2 | 176.4 | 3.68 | 156.1 |
| 19 | | −64.3 | −63.3 | −139.0 | 141.4 | 137.5 | 2.38 | 173.6 | 120.2 | 154.0 | 2.73 | 165.9 |
| 20 | | −63.5 | −63.5 | −138.8 | 141.1 | 137.9 | 2.38 | 173.6 | 120.9 | 154.1 | 2.73 | 165.8 |
| 21 | | −52.7 | −74.6 | −143.4 | −75.6 | −175.6 | 2.41 | 176.0 | 118.6 | −145.4 | 4.71 | 44.5 |
| 22 | anti | −179.4 | 83.7 | −163.4 | −104.9 | 18.7 | 2.35 | 175.0 | 123.9 | 29.9 | 2.65 | 172.9 |
| 23 | | −175.6 | 67.5 | −163.4 | 66.8 | −147.8 | 2.35 | 175.3 | 121.8 | 25.7 | 2.65 | 166.5 |
| 24 | | −176.5 | 69.0 | −163.6 | 66.5 | −147.7 | 2.35 | 175.3 | 121.7 | 24.3 | 2.65 | 166.7 |
| 25 | | −176.3 | 69.1 | −162.3 | −113.9 | 32.9 | 2.35 | 175.5 | 121.8 | 24.5 | 2.65 | 166.5 |
| 26 | | −176.2 | 68.3 | −163.6 | 66.8 | −148.1 | 2.35 | 175.3 | 121.7 | 25.0 | 2.65 | 166.5 |
| 27 | | −177.9 | 79.9 | −164.4 | 75.3 | −160.9 | 2.35 | 175.0 | 123.5 | 33.8 | 2.65 | 172.7 |
| 28 | | −177.9 | 80.2 | −164.3 | 75.4 | −160.7 | 2.35 | 174.8 | 123.6 | 32.9 | 2.65 | 172.8 |

For definitions of energy values, see text and Table 1, footnote d.
[a] See Fig. 4 for the definition of $\tau_1$–$\tau_5$; given in [c].
[b] Subscript (A) denotes $Asp^{186}$.
[c] Subscript (T) denotes $Tyr^{182}$ or $Thr^{190}$.
[d] In au.
[e] In kcal/mol; the au to kcal/mol conversion factor equals 627.509541 (taken from Ref. 29).

the H-bond geometry being closest to X-ray data without regarding total energy values. In total, 28 conformations were selected, which function as starting geometries for the ab initio analysis of histamine interacting with the oligopeptide via H-bonds.

*Further simplification of the model system; Hartree–Fock geometry optimization (Fig. 3, step 5)* For each of the 28 selected conformations, a geometry optimization was performed at the Hartree–Fock (HF) level (no. **5** in the flow chart, Fig. 3). Because these ab initio calculations are computationally demanding, the above-mentioned decapeptide was divided into two simplified pentapeptides consisting of: (a) Tyr-Gly-Gly-Gly-Asp; and (b) Asp-Gly-Gly-Gly-Thr.

In order to keep the α-helix mimicking parts as simple as possible, all amino acids in between the essential ones were replaced by Gly, while preserving the preset α-helical φ/ψ angles. Additional computational efficiency is achieved by replacing the histamine molecule by 5-methylimidazole. Changing histamine into 5-methylimidazole is a generally accepted approximation (e.g. Refs. 1 and 3) and is validated by the fact that the positively charged side chain of histamine interacts with the negatively charged aspartic acid from TM3 ($Asp^{98}$). The resulting HF geometries and interaction energies were analysed to extract the best-possible interaction modes.

All ab initio geometry optimizations were performed at the HF level using a minimal STO-3G basis set [21–24, and references cited therein], expecting a certain amount of fortuitous cancellation of errors for the resulting geometries [25]. Since all separate molecules and complexes possess an even number of electrons, we have chosen the spin-restricted HF method (i.e. all electrons are divided into pairs with opposite spin – α, β – and each pair oc-

| $H_{(T)}...N^{\tau}-C_2$ | $E_{total}$ oligo + ligand (6-31G*)[d] | $E_{intra}$ oligo (6-31G*; FCP)[d] | $E_{intra}$ ligand (6-31G*; FCP)[d] | $E_{inter}$ (6-31G*; FCP)[e] | $E_{intra}$ oligo (6-31G*)[d] | Relative $E_{intra}$ oligo (strain) (6-31G*)[e] | Strain-corrected $E_{inter}$ (6-31G*)[e] |
|---|---|---|---|---|---|---|---|
| 112.3 | −1752.9130 | −1489.0414 | −263.8508 | −13.05 | −1489.0356 | 23.66 | 10.61 |
| 112.5 | −1752.9119 | −1489.0403 | −263.8509 | −12.99 | −1489.0348 | 24.16 | 11.17 |
| 112.7 | −1752.9129 | −1489.0415 | −263.8508 | −12.93 | −1489.0357 | 23.59 | 10.66 |
| 112.3 | −1752.9131 | −1489.0414 | −263.8508 | −13.11 | −1489.0356 | 23.66 | 10.55 |
| 40.7 | −1752.9242 | −1489.0616 | −263.8493 | −8.35 | −1489.0560 | 10.86 | 2.51 |
| 36.7 | −1752.9188 | −1489.0543 | −263.8490 | −9.37 | −1489.0493 | 15.06 | 5.69 |
| 57.1 | −1752.9227 | −1489.0584 | −263.8498 | −9.10 | −1489.0529 | 12.80 | 3.70 |
| 96.3 | −1752.9242 | −1489.0603 | −263.8517 | −7.66 | −1489.0543 | 11.92 | 4.26 |
| 84.2 | −1752.9260 | −1489.0670 | −263.8491 | −6.21 | −1489.0634 | 6.21 | 0.00 |
| 101.0 | −1752.9283 | −1489.0608 | −263.8508 | −10.48 | −1489.0551 | 11.42 | 0.94 |
| 96.0 | −1752.9242 | −1489.0600 | −263.8517 | −7.84 | −1489.0541 | 12.05 | 4.21 |
| 49.4 | −1752.9298 | −1489.0691 | −263.8494 | −7.09 | −1489.0650 | 5.21 | −1.88 |
| 79.4 | −1752.9281 | −1489.0681 | −263.8490 | −6.90 | −1489.0647 | 5.40 | −1.50 |
| 120.3 | −1752.9156 | −1489.0586 | −263.8509 | −3.83 | −1489.0531 | 12.68 | 8.85 |
| 116.6 | −1943.4291 | −1679.5497 | −263.8511 | −17.76 | −1679.5438 | 13.30 | −4.46 |
| 118.0 | −1943.4046 | −1679.5217 | −263.8511 | −19.95 | −1679.5163 | 30.56 | 10.61 |
| 121.9 | −1943.4190 | −1679.5360 | −263.8512 | −19.95 | −1679.5275 | 23.53 | 3.58 |
| 104.8 | −1943.4371 | −1679.5682 | −263.8501 | −11.80 | −1679.5636 | 0.89 | −10.91 |
| 116.5 | −1943.4291 | −1679.5498 | −263.8511 | −17.70 | −1679.5439 | 13.24 | −4.46 |
| 116.4 | −1943.4294 | −1679.5502 | −263.8511 | −17.63 | −1679.5444 | 12.93 | −4.70 |
| 75.6 | −1943.4227 | −1679.5629 | −263.8496 | −6.40 | −1679.5581 | 4.33 | −2.07 |
| 118.2 | −1943.4200 | −1679.5370 | −263.8515 | −19.78 | −1679.5310 | 21.34 | 1.56 |
| 126.4 | −1943.4163 | −1679.5356 | −263.8514 | −17.13 | −1679.5298 | 22.09 | 4.96 |
| 126.4 | −1943.4162 | −1679.5374 | −263.8515 | −17.13 | −1679.5296 | 22.21 | 5.08 |
| 126.5 | −1943.4163 | −1679.5354 | −263.8514 | −18.20 | −1679.5296 | 22.21 | 4.01 |
| 126.4 | −1943.4162 | −1679.5355 | −263.8514 | −18.39 | −1679.5297 | 22.15 | 3.76 |
| 118.2 | −1943.4205 | −1679.5374 | −263.8515 | −19.83 | −1679.5314 | 21.08 | 1.25 |
| 118.4 | −1943.4204 | −1679.5374 | −263.8515 | −19.78 | −1679.5314 | 21.08 | 1.30 |

cupies the same spatial molecular orbital) throughout all ab initio calculations. Geometry optimizations were performed using the recommended quasi-Newton rank-2 update procedure with default convergence criteria invoked (maximum change in the variables $< 0.003$, average change in the variables $< 0.002$, maximal gradient $< 0.0013$, and average gradient $< 0.00089$; Refs. 22–24). Once converged, all geometry optimizations were followed by single-point 6-31G* energy calculations in order to compare the relative, more accurate, ab initio energies. The calculation of the interaction energy between the 5-methylimidazole and the respective oligopeptides (a) and (b) will be addressed in the subsequent subsection. Throughout, the quantum chemical programme package GAMESS-UK [21–23] was used on a Cray-C98 supercomputer.

The geometry of the 5-methylimidazole fragment was taken from the X-ray structure of histamine [16]; only the hydrogen positions – in general not reliably determined in an X-ray study – were optimized in a separate HF/STO-3G calculation. Then the supermolecule was optimized with the same flexibility as allowed in the molecular mechanics optimizations, except for the tyrosine and threonine H-O-C valence angles, which were added to the variables (see Fig. 4). Finally, the separate oligopeptide was optimized in an HF/STO-3G calculation starting from its Chem-X global minimum in the absence of the histamine fragment. It is assumed that in this way the ab initio (HF/STO-3G) geometry of the global minimum of the pentapeptide is determined. This information can then be used to correct the interaction energy for strain in the oligopeptide induced by the ligand (Table 4).

*Basis set superposition error, calculation of interaction energies (Fig. 3, step 6)* Since the basis set superposition error (BSSE) artificially enhances the ab initio interaction energies (e.g. Ref. 24, and references cited therein), the Boys and Bernardi counterpoise (CP) method [26] was applied to eliminate this BSSE. Gutowski et al. [27] demonstrated that the CP recipe indeed yields interaction energies that correspond precisely to the basis set and correlation method applied in the ab initio calculation at hand. This counterpoise method involves the calculation of the energies of the entities constituting the supermolecule and the supermolecule itself in the basis set applied

to the supermolecule (no. **6** in the flow chart, Fig. 3). The basis set of the entire complex is used at all stages and for all (sub)systems. So, an energy calculation on the pentapeptide also included the orbitals of the ligand; the latter are called 'ghost orbitals': where the atoms of the ligand are absent, they are mimicked by so-called 'ghost atoms', which have no charge but only atomic orbitals. An energy calculation on the ligand also included the oligopeptide's orbitals. The interaction energy was obtained from the energy of the entire complex minus the sum of the energy values of the subsystems (calculated in the supermolecule orbital basis).

The obtained interaction energies must be corrected for strain in the oligopeptide induced by ligand binding. For this purpose, the energy of the oligopeptide entity – with the same geometry as present in the selected minima of the entire complex – was calculated in a 6-31G* basis set of the monomer, i.e. without considering the orbitals of the ligand. This allows for a comparison between the global minimum HF/6-31G*//STO-3G energy (i.e. single-point energy calculation in the 6-31G* basis set after an STO-3G geometry optimization) of the oligopeptide (Table 3) and the HF/6-31G* energy of the peptide as present in the complex. The difference is referred to as the strain energy. The strain-corrected interaction energy is obtained by subtracting the strain energy from the BSSE-corrected interaction energy [24].

These ab initio calculations will allow one to predict whether, in general, a 5-methylimidazole moiety in its proximal tautomeric form is more likely to bind to an α-helical oligopeptide containing a Tyr and an Asp separated by three amino acids (not being a proline) or to a similar oligopeptide containing an Asp and a Thr at corresponding positions. The calculations will also reveal whether the imidazole can indeed interact via the two predicted H-bonds.

## Results and Discussion

*Chem-X results, Tables 1 and 2*

The Chem-X [11] molecular mechanics results obtained from the conformational search with subsequent optimization (Fig. 3, steps **1–3**) are summarized in Table 1. The intramolecular energy of the oligopeptide within a subset of 28 complex conformations ($E_{intra}$ oligo, Table 1) is given *relative* to the global minimum of the peptide, i.e. either the lowest energy of the Tyr/Asp binding site or the Asp/Thr binding site (Table 2, vide infra). The 28 minima depicted in Table 1 have been selected (Fig. 3, step **4**) on the basis of both optimal intermolecular energy values and on the best resemblance with the average geometrical H-bond data, which have emerged from a large number of proteins [17]. Some of the found geometries seem equal (**3** and **4**; **5–7**; **8** and **11**; **9** and **12–14**; **19** and **20**; **22** and **25**; **23** and **26–28**, Table 1), but for reasons outlined above (Methods section), all 28 conformations have subsequently been optimized at the HF/STO-3G level (Fig. 3, step **5**; vide infra).

Only for the syn-Tyr/Asp interaction a negative (i.e. attractive) value for the strain-corrected molecular mechanics interaction energy was found (Table 1, strain-corrected $E_{inter}$ for no. **15**). This implies that the histamine-induced strain energy in the oligopeptide can be overcome by the interaction energy. Considering just energetics, we conclude from these Chem-X results that the tyrosine–aspartate interaction (syn) looks most promising.

The discrepancies between the average H-bonds as given by Ippolito *et al.* [17] and the ones found for the histamine binding modes are represented by the $\Sigma\Delta_{dum}$ values. Considering geometries, the anti-aspartate/threonine binding comes closest to the average X-ray H-bond geometry (minima **9** and **12–14**). However, large variations in the energy values for these geometries were observed, although the conformations are quite similar. These large variations in energies for the geometries found originate from the rather large restraint forces used in the Chem-X optimization procedure.

Finally, Table 1 presents the resulting Chem-X H-bond geometries. The H-bond distances between the hydrogen-donating proximal nitrogen of histamine and the accepting oxygen of $Asp^{186}$ ($N^{\pi}...O_{(A)}$) are close to the biased 2.9 Å; this also holds for the distance between the proton-donating $Thr^{190}/Tyr^{182}$ and the alkaline tele-nitrogen of histamine ($O_{(T)}...N^{\tau}$). The largest deviation of 0.4 Å was found for the $N^{\pi}...O_{(A)}$ distance in no. **17**, resulting in a favourably shorter H-bond. All H-bond distances are smaller than 3.5 Å, so that all resulting geometries are able to form H-bonds when only the hydrogen bond distance is considered. The $N^{\pi}$-$H^{\pi}...O_{(A)}$ and $O_{(T)}$-$H_{(T)}...N^{\tau}$ angles can be considered as optimal when they are close to 180°. The largest deviations were found for minima **16** and **17**, i.e. 51° and 60°, respectively. From the HF/STO-3G optimization of the isolated 5-methylimidazole fragment it is known that the optimal valence angle for H-$N^{\pi}$-$C_2$ equals 126.4°. Given the value of this angle and the symmetry of the imidazole with respect to the $N^{\pi}$-$C_2$ and $C_2$-$N^{\tau}$ bonds, minimum **5** displays the largest deviation (108.8° instead of 126.4°). Syn-interactions in the plane of the carboxylate (minima **1–7** and **15–21**) are optimal at $H^{\pi}...O_{(A)}$-$C_{(A)}$-$C_{(A)}$ angles of ± 180°, whereas anti-interactions (minima **8–14** and **22–28**) should be close to 0°. The largest discrepancy of about 20° from a pure syn-interaction in the carboxylate plane is found for minima **16** and **17** (N.B.: these minima also reveal large deviations from an optimal $N^{\pi}$-$H^{\pi}...O_{(A)}$ angle; see above). All other minima (both syn and anti) can form H-bonds between the imidazole and the aspartic acid within 7° of the carboxylate plane.

Table 2 displays the molecular mechanics data of the (Chem-X) global minima for the Tyr/Asp and Asp/Thr

binding site. During these geometry optimizations, no restraint forces were applied. The intramolecular energy of these global minima was the reference for calculating the strain energy induced by the ligand upon binding to the peptide ($E_{intra}$ oligo, Table 1). $Thr^{190}$ is hydrogen-bonded to the α-helical backbone, which explains the large deviation of 48° in $\tau_4$ from the staggered minimum (180°).

*Ab initio (HF) results, Tables 3 and 4*

Table 3 contains results of the HF/6-31G*//STO-3G calculations on the global minima obtained with Chem-X for both binding site couples Tyr/Asp and Asp/Thr (Table 2). In Fig. 9, this ab initio global minimum for the Asp/Thr couple in the absence of the ligand is depicted. The values for both $\tau_2$ and $\tau_4$ differ significantly from the molecular mechanics data (cf. Tables 2 and 3). Figure 9 shows the presence of an H-bond which is formed between the $Thr^{190}$ hydroxyl and a C=O backbone group, and the coupling of the negatively charged $Asp^{186}$ in line with the dipole moment of the α-helical pentapeptide. Both $\tau_1$ and $\tau_3$ are close to the staggered minimum-energy values of –60 and 60, respectively.

Table 3 also presents the ab initio data for the global minimum of the Tyr/Asp binding site. Within this pentapeptide an H-bond between $Tyr^{182}$ and $Asp^{186}$ is observed. This interaction is responsible for the large deviation of $\tau_5$ from the phenolic plane (–115.8°; a value of 0° or ± 180° is expected for a pure $sp^2$ OH group). The dihedrals $\tau_1$ and $\tau_2$ largely differ from the respective Chem-X values. These differences are ascribed to the absence of directionality in Chem-X H-bonds.

Table 4 summarizes the ab initio results for the 28 selected Chem-X minima of the complex. The highest absolute interaction energies ($E_{inter}$) of about 20 kcal/mol were found for the interaction with the Tyr/Asp binding site (nos. **16**, **17**, **22**, **27** and **28**). In contrast, the interaction with the Asp/Thr binding site does not yield more than 13 kcal/mol (nos. **1**–**4**). More importantly, the strain-corrected interaction energies (strain-corrected $E_{inter}$) are in general more favourable for the Tyr/Asp couple (see e.g. **15** and **18**–**21**) than for the Asp/Thr interaction, although not always two optimal H-bonds are formed: the $O_{(T)}...N^{\tau}$ distance is as large as 3.7 Å for minimum **18**, and 4.7 Å for **21**. From now on, the strain-corrected interaction energy is referred to as the interaction energy. However, also for the Asp/Thr interaction, two negative (i.e. attractive) interaction energies were observed (**12** and **13**), so that a possible interaction with the Asp/Thr binding site cannot be rejected fully based on interaction energy arguments only. The most favourable Asp/Thr bonding interactions can be seen to occur anti with respect to the carboxylate (**12** and **13**), whereas the Tyr/Asp bonding interactions appear syn with respect to the same carboxylate (**15** and **18**–**21**).

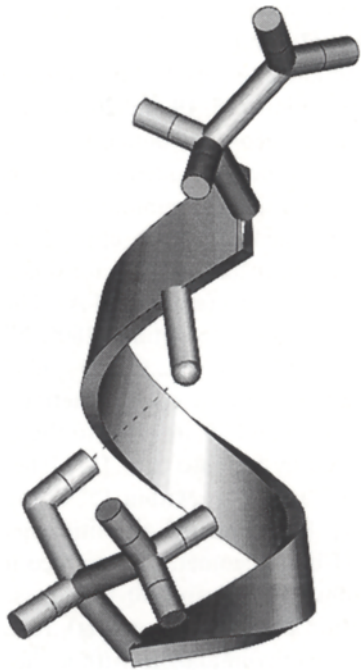

Fig. 9. Global minimum for the α-helical D-G-G-G-T pentapeptide obtained after Chem-X [11] and subsequent HF/STO-3G geometry optimization. The α-helical configuration is stabilized by the H-bond (dotted line) between the hydroxyl group of $Thr^{190}$ and a C=O peptide backbone group. The negatively charged carboxylate group couples in line with the dipole moment of the α-helix. The picture was made with the programme SETOR, v. 4.13.4 (University of British Columbia [28]).

Table 4 also presents the H-bond geometries resulting from the ab initio geometry optimizations. Investigating the distances between the H-bonded heteroatoms, it is evident that the complexes **5**–**7**, **9**, **12**, **13** and **21** are not able to establish two acceptable H-bonds between the imidazole moiety and the oligopeptide. For all these conformations the distance between the participating heteroatoms is larger than 4 Å. Since only **12** and **13** possess negative interaction energies, it seems impossible for the Asp/Thr couple to accommodate an imidazole ring system with two acceptable H-bonds at the same time. On the other hand, minima **15** and **18**–**20** represent likely binding modes for histamine to the Tyr/Asp couple in case only interaction energies and acceptable H-bond distances are considered. For **18**, the largest absolute interaction energy is found (–10.91 kcal/mol). The $N^{\pi}...O_{(A)}$ distance of 2.38 Å in **18** is very short, demonstrating that the electrostatic interactions in the gas phase are very tight. The $N^{\pi}$-$H^{\pi}...O_{(A)}$, $N^{\pi}...O_{(A)}$-$C_{(A)}$ and $H^{\pi}...O_{(A)}$-$C_{(A)}$-$C_{(A)}$ in **18** are within 5° from their optimal values, showing that the imidazole carboxylate H-bond is close to its optimum. The second H-bond in **18** reveals a rather large distance (3.68 Å) between the hydroxyl oxygen ($O_{(T)}$) and $N^{\tau}$. The $O_{(T)}$-$H_{(T)}...N^{\tau}$ and $H_{(T)}...N^{\tau}$-$C_2$ angles are within 25° from their optimal values. However, based on the rather large HF/STO-3G distance between the $O_{(T)}$ and $N^{\tau}$ conforma-

tion **18**, this Tyr–imidazole interaction cannot be regarded as a significant H-bond.

The interaction energies for histamine to the other three Tyr/Asp minima (**15**, **19** and **20**) are all close to –4.5 kcal/mol. From the geometry data on $\tau_1$–$\tau_5$ and the resulting H-bonds, it can be concluded that minima **15**, **19** and **20** represent the same local minimum (mutual deviations are within convergence criteria applied during the ab initio geometry optimization). Also for this minimum, the distance $N^{\pi}...O_{(A)}$ is short (almost 2.4 Å). The $N^{\pi}$-$H^{\pi}...O_{(A)}$ angle is within 6° from the optimal 180°, $N^{\pi}...O_{(A)}$-$C_{(A)}$ is within 1° from 120°, and $H^{\pi}...O_{(A)}$-$C_{(A)}$-$C_{(A)}$ deviates approximately 26° from a pure syn-interaction. The $O_{(T)}...N^{\tau}$ distances for **15**, **19** and **20** are close to the X-ray value of 2.9 Å as reported by Ippolito et al. [17]. The $O_{(T)}$-$H_{(T)}...N^{\tau}$ and $H_{(T)}...N^{\tau}$-$C_2$ angles are within 15° of the reported X-ray values [17]. Based on the ab initio energy data and the resulting H-bond geometries presented in Table 4, we conclude minima **15**, **19** and **20** to represent the same minimum (within convergence criteria), revealing a binding mode of 5-methylimidazole within the oligopeptide which consists of two H-bonds (Fig. 10). Thus, in contrast with the Asp/Thr binding site, the Tyr/Asp couple can bind 5-methylimidazole with two acceptable H-bonds and an attractive energy.

Overall, the HF/STO-3G $N^{\pi}...O_{(A)}$ distances were seen to be close to 2.4 Å. This distance is significantly smaller than the mean X-ray value of 2.9 Å as given by Ippolito et al. [17], and is due to the gas-phase character of the calculations. In addition, the minimal STO-3G basis set applied in the ab initio geometry optimizations (Fig. 3, step **5**) lacks diffuse functions on the oxygen atoms in the negatively charged carboxylate, which slightly contributes to these small distances as well. The characteristic features of the CP method are illustrated by differences in intramolecular energies for the ligand ($E_{intra}$ ligand, Table 4): although the geometry of the ligand was fixed during the HF/STO-3G geometry optimization, its (CP) intramolecular energy depends on the conformation of the pentapeptide, and different conformations of the peptide result in different contributions to the CP energy of the ligand. Note that the geometry optimizations were done without CP.

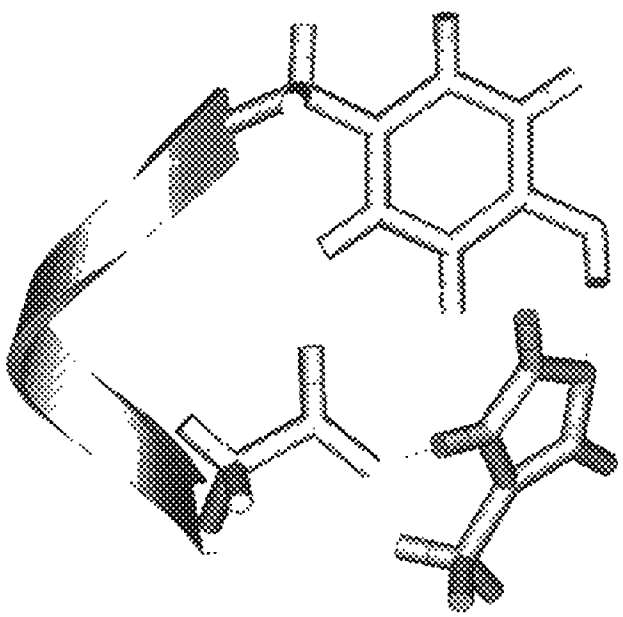

Fig. 10. Interaction via two H-bonds of 5-methylimidazole with the α-helical Y-G-G-G-D pentapeptide (Chem-X [11] and subsequent HF/STO-3G geometry optimization; no. **20** from Table 4 is depicted). The picture was made with SETOR [28].

In Table 4, the largest absolute deviation of $\tau_1$ from a nearby Newman minimum was found for **11**, i.e. |38.9°| from its Newman minimum at –60°. The optimal histamine interaction in minima **15**, **19** and **20** occurs with a $\tau_1$ value of –64°, which deviates approximately 25° from the global minimum value of 89.9° for the oligopeptide (Table 3). Since $\tau_1$ is assigned to the dihedral $C_{(backbone)}$-$C^{\alpha}$-$C^{\beta}$-$C^{\gamma}$, the above implies that histamine binding to the global minimum of the Tyr/Asp binding site hardly influences the direction of $C^{\gamma}$ of $Asp^{186}$. Dihedral $\tau_2$, on the contrary, can deviate to a much larger extent from its local minimum; $\tau_2$ can even be close to a Newman maximum eclipsed conformation (see no. **18**). Minimum **18** illustrates furthermore that the strain induced in $\tau_2$ by the interaction of the imidazole moiety with the carboxylate group can be overcome by intermolecular interactions (strain-corrected $E_{inter} = -10.9$ kcal/mol). The largest deviation from a Newman $\tau_3$ value was found for **15**, **19** and **20**, being approximately 40°. As already noticed for $\tau_1$, the optimal histamine interaction in minima **15**, **19** and **20** is seen to occur at a $\tau_3$ value of 139°, which is approximately the same structure (considering the $\tau_3$ value) as found for the global minimum of the Tyr/Asp binding site (173.9°, Table 3). For $\tau_4$ in $Thr^{190}$, the largest discrepancy from an $sp^3$-$sp^3$ minimum was observed for **14** (33.1°). For $\tau_4$ in Tyr, the largest deviation from an optimal $sp^3$-$sp^2$ value was found for **24** (23.5°). Finally, $\tau_5$ was seen to deviate from planarity by at most 42.6° (**15**). (N.B.: A $\tau_5$ of 0 or ±180° and a C-O-H valence angle of 120° indicate a pure $sp^2$ phenolic oxygen, whereas an out-of-plane bending value for $\tau_5$ and a C-O-H valence angle close to 109° indicate an $sp^3$ hybridization for the phenolic oxygen.) The investigated $sp^3$-$sp^2$ bonds can be closer to Newman maxima than the $sp^3$-$sp^3$ bonds, which suggests that the rotation barriers for the studied $sp^3$-$sp^3$ bonds are higher than for the $sp^3$-$sp^2$ bonds. The phenolic oxygen of $Tyr^{182}$ was found to have a predominant $sp^3$ character in minima **15**, **19** and **20**, since the C-O-H valence angle is 105.4° (not shown) and $\tau_5$ displays an out-of-plane bending of more than 40° (Table 4). In conformation **21**, $\tau_5$ deviates only 4.4° from planarity; however, the C-O-H valence angle equals 105.4°. Therefore, we conclude that in complex **21** the phenolic oxygen has a mixed $sp^2/sp^3$

character, which also holds for complexes **16** and **22**, which have the highest valence angle values found in the series (107.8°) and an out-of-plane bending of approximately 20°. The oxygen of $Thr^{190}$ has a pure $sp^3$ character, with valence angles in the range of 103.7 (nos. **2–5**) to 111.3° (no. **14**).

## Conclusions

*Evidence for the involvement of $Tyr^{182}$ and $Asp^{186}$ in histamine binding*

From the results described in the previous section, we conclude that histamine rather interacts with the $Tyr^{182}$/$Asp^{186}$ couple than with the earlier suggested [2] $Asp^{186}$/$Thr^{190}$. Neglecting the strain imposed upon the oligopeptide by ligand binding, the interaction of the histamine with the Tyr/Asp couple is 7 kcal/mol more favourable than with the Asp/Thr binding site (ab initio data). In case the intramolecular strain energy of the oligopeptide is taken into account, the ab initio calculations indicate the Tyr/Asp interaction to be up to 9 kcal/mol more favourable than the Asp/Thr interaction. Within the Tyr/Asp binding site, the histamine imidazole system is able to achieve an overall energy gain by forming one (minimum **18**) as well as two H-bonds (minima **15**, **19** and **20**) with $Tyr^{182}$ and $Asp^{186}$ simultaneously; within the Asp/Thr binding site, only one hydrogen bond can be formed (with $Asp^{186}$) in those cases where an attractive (strain-corrected) interaction energy is observed. In the literature [1–5,30], the histamine interaction with TM5 of the histamine $H_2$ receptor is predicted to occur via two simultaneous H-bonds. Only the Tyr/Asp binding site can accommodate the two H-bonds. These conclusions are all based on enthalpic considerations. The entropic component of ligand binding is not regarded in the present calculations. In general, H-bond formation leads to a loss in entropy. Hence, in case, already at the enthalpic level, two simultaneous H-bonds with $Asp^{186}$/$Thr^{190}$ cannot be formed, including the entropy will not affect this finding. Therefore, we consider the $Tyr^{182}$/$Asp^{186}$ couple to be the only candidate at TM5 for binding histamine via two H-bonds.

It is noted that the H-bonds presented in Table 1 and obtained after Chem-X optimization of the various complexes all have reasonable acceptor–donor distances and display the correct angular behaviour. Hence, H-bond biasing in molecular mechanics with the aid of dummy atoms and restraint forces is a very useful ad hoc method in order to get more reasonable hydrogen bond geometries from the applied (minimal) force field. The recommended value of 100 for the force constants favours H-bonds; however, the energy values of the geometries found cannot be trusted (Table 1, vide supra). The generated molecular mechanics minima do nevertheless provide excellent start geometries for subsequent ab initio calculations.

Hydroxyl groups of threonine residues are generally observed to be involved in hydrogen bonds with C=O backbone atoms in an α-helical configuration. The presence of a methyl group at the $C^{\beta}$ side-chain atom of Thr probably facilitates this C=O backbone H-bonding. As a consequence, the mutation of $Thr^{190}$ could destabilize (parts of) the fifth α-helix, resulting in a different relative orientation of amino acids (obstructing/inhibiting agonist binding). In the global minimum of the Asp/Thr binding site, $Thr^{190}$ is indeed seen to interact with the receptor backbone (Fig. 9), and the unfavourable effect of altering $Thr^{190}$ on histamine binding and receptor stimulation can very well be explained via an indirect role.

Both in molecular mechanics and in subsequent ab initio calculations, the Tyr/Asp binding site is seen to be favourable for the syn-orientated interaction of histamine with respect to the carboxylate group of $Asp^{186}$. This leads to a close resemblance of the histamine binding site with a structure already found in nature, the catalytic triad in serine proteases, consisting of a Ser, His and Asp residue [6,7, and references cited therein].

*The catalytic triad of serine proteases as a model for the histamine $H_2$ receptor agonistic binding site at TM5*

Within the X-ray structures of the serine proteases, the carboxylate group of the catalytic triad is found to interact in a syn-orientation with the histidine having its imidazole ring in the proximal tautomeric form [31]. The negatively charged Asp is thought to lower the activation barrier for the essential step: a proton abstraction from the hydroxyl group of the serine residue [6,7,32]. Subsequently, this proton moves from the serine towards the tele-side of the histidine's imidazole ring system [6,7,32]. A subsequent proton transfer from the resulting positively charged histidine towards the negatively charged carboxylate of the triad's aspartate has seriously been questioned (e.g. Ref. 7). The relative orientation of the amino acids interacting with the imidazole ring of histamine at the agonistic binding site of the histamine $H_2$ receptor resembles that of the residues constituting the catalytic triad in serine proteases. However, their nature differs: a tyrosine instead of a serine is found in the putative agonistic binding site at the fifth transmembrane domain of the histamine $H_2$ receptor. The doubts raised with respect to a proposed proton transfer from the histidine in the catalytic triad towards the negatively charged carboxylate [7] are in line with our earlier suggestions that the role of $Asp^{186}$ in the histamine $H_2$ receptor is mainly electrostatic [3]. Hence, in this way, it is understandable that the $Asp^{186}$ to $Ala^{186}$ mutant displays a reduced, yet still significant, cAMP response upon histamine stimulation. The syn-orientated interaction between an imidazole ring and a carboxylate group has been shown to have a stronger alkaline character than the anti-orientated binding [17]. Thus, both in serine proteases and in the $Tyr^{182}$/$Asp^{186}$ binding

site of the histamine $H_2$ receptor, the negative charge of the syn-orientated carboxylate is optimally used.

*Deletion model for the origin of receptors*

Topiol [33] postulated a deletion model for the origin of receptors: receptors, together with their agonists, are regarded to be derived from a common parent system. This system is a collection of entities necessary for the function of a complete dynamic biological system. The absence of one entity ($\alpha_1$ subunit) generates an inactive subsystem. Only when the $\alpha_1$ subunit and the inactive subsystem are recombined does activity return. The relationship between endogenous ligands and amino acids, for example histamine and histidine, respectively, follows directly from this model. This deletion model provides an obvious possibility for relating the catalytic triad as present in serine proteases with the agonistic binding site of the histamine $H_2$ receptor: histamine, when bound to the histamine $H_2$ receptor, can fulfil the same role as the histidine in the catalytic triad, i.e. accepting a proton at the tele-position of the imidazole ring system.

## Acknowledgements

We express our gratitude to Dr. Luc Koymans and Ing. Henry Moereels for very valuable discussions and the kind hospitality experienced during the visits to the Janssen Research Foundation. The investigations were supported in part (P.H.J.N.) by the Netherlands Foundation for Chemical Research (SON) with financial aid from the Netherlands Organization for Scientific Research (NWO). This work was generously sponsored by the Stichting Nationale Computerfaciliteiten (National Computing Facilities Foundation, NCF) with financial support from the Nederlandse Organisatie voor Wetenschappelijk Onderzoek (the Netherlands Organization for Scientific Research, NWO).

## References

1 Weinstein, H., Mazurek, A.P., Osman, R. and Topiol, S., Mol. Pharmacol., 29 (1986) 28.
2 Gantz, I., DelValle, J., Wang, L., Tashiro, T., Munzert, G., Guo, Y.-J., Konda, Y. and Yamada, T., J. Biol. Chem., 267 (1992) 20840.
3 Nederkoorn, P.H.J., Vernooijs, P., Donné-Op den Kelder, G.M., Baerends, E.J. and Timmerman, H., J. Mol. Graph., 12 (1994) 242.
4 Eriks, J.C., Van der Goot, H. and Timmerman, H., Mol. Pharmacol., 44 (1993) 886.
5 Nagy, P.I., Durant, G.J., Hoss, W.P. and Smith, D.A., J. Am. Chem. Soc., 116 (1994) 4898.
6 Carter, P. and Wells, J.A., Nature, 332 (1988) 564.
7 Warshel, A., Naray-Szabo, G., Sussman, F. and Hwang, J.-K., Biochemistry, 28 (1989) 3629.
8 Gantz, I., Munzert, G., Tashiro, T., Schäffer, M., Wang, L., DelValle, J. and Yamada, T., Biochem. Biophys. Res. Commun., 178 (1991) 1386.
9 Zubay, G., In Biochemistry, Wm. C. Brown Publishers, Dubuque, IA, U.S.A., 1993.
10 Bashford, D. and Karplus, M., Biochemistry, 29 (1990) 10219.
11 Chem-X Reference Guide, Chemical Design Ltd., Oxon. U.K., July 1994.
12 Darbey, N.J. and Creighton, T.E., In Rickwood, D. (Ed.) Protein Structure, IRL Press, Oxford, U.K., 1993, pp. 1–22.
13 Oliveira, L., Paiva, A.M.C. and Vriend, G., J. Comput.-Aided Mol. Design, 7 (1993) 649.
14 Némethy, G. and Scheraga, H.A., Rev. Biophys., 10 (1977) 239.
15 Vriend, G. and Eijsink, V., J. Comput.-Aided Mol. Design, 7 (1993) 367.
16 Cambridge Structural Database; Refcode hisahc10: Bonnet, J.J., Jeannin, Y. and Laaouini, M., Bull. Soc. Fr. Miner. Cri., 98 (1975) 208.
17 Ippolito, J.A., Alexander, R.S. and Christianson, D.W., J. Biol. Chem., 215 (1990) 457.
18 Del Re, G., Gavuzzo, E., Giglio, E., Lelj, F., Mazza, F. and Zappia, V., Acta Crystallogr., B33 (1977) 3289.
19 Van Duijneveldt-Van de Rijdt, J.G.C.M. and Van Duijneveldt, F.B., J. Am. Chem. Soc., 93 (1971) 5644.
20 Smit, P.H., Derissen, J.L. and Van Duijneveldt, F.B., J. Chem. Phys., 67 (1977) 274.
21 GAMESS-UK is a package of ab initio programmes written by Guest, M.F., Van Lenthe, J.H., Kendrick, J., Schoeffel, K., Sherwood, P. and Harrison, R.J., with contributions from Amos, R.D., Buenker, R.J., Dupuis, M., Handy, N.C., Hillier, I.H., Knowles, P.J., Bonacic-Koutecky, V., Von Niessen, W., Saunders, V.R. and Stone, A.J. The package is derived from the original GAMESS code, see Ref. 22.
22 Dupuis, M., Spangler, D. and Wendoloski, J., GAMESS, Natural Resource of Computational Chemistry Software Catalog, Vol. 1, Program No. QG01, 1980.
23 Guest, M.F., Fantucci, P., Harrison, R.J., Kendrick, J., Van Lenthe, J.H., Schoeffel, K. and Sherwood, P., GAMESS-UK User's Guide and Reference Manual, CFS Ltd., Daresbury Laboratory, Daresbury, U.K., 1993.
24 Van Lenthe, J.H., Van Duijneveldt-Van de Rijdt, J.G.C.M. and Van Duijneveldt, F.B., In Lawley, K.P. (Ed.) Ab Initio Methods in Quantum Chemistry, Wiley, New York, NY, U.S.A., 1987, pp. 521–565.
25 Kolos, W., Theor. Chim. Acta, 54 (1980) 187.
26 Boys, S.F. and Bernardi, F., Mol. Phys., 19 (1970) 553.
27 Gutowski, M., Van Duijneveldt-Van der Rijdt, J.G.C.M., Van Lenthe, J.H. and Van Duijneveldt, F.B., J. Chem. Phys., 98 (1993) 4728.
28 Evans, S.V., J. Mol. Graph., 11 (1993) 134.
29 Pyykkoe, P. and Zhao, Y., Report HUKI, 1 (1989) 89.
30 Sippl, W., Stark, H. and Höltje, H.-D., Quant. Struct.–Act. Relatsh., 14 (1995) 121.
31 Marquart, M., Walter, J., Deisenhofer, J., Bode, W. and Huber, R., Acta Crystallogr., B39 (1983) 480.
32 Daggett, V., Schröder, S. and Kollman, P., J. Am. Chem. Soc., 113 (1991) 8926.
33 Topiol, S., Trends Biochem. Sci., 12 (1987) 419.